

A Data-Centric Approach to Pedestrian Attribute Recognition: Synthetic Augmentation via Prompt-driven Diffusion Models

Alejandro Alonso^{1,2,3}, Sawaiz A. Chaudhry^{1,2,3}, Juan C. SanMiguel¹,
 Álvaro García-Martín¹, Pablo Ayuso-Albizu¹, Pablo Carballeira¹

¹Autonomous University of Madrid, Madrid, Spain. ²University of Bordeaux, Bordeaux, France.

³Pázmány Péter Catholic University, Budapest, Hungary.

{alejandro.alonsog, sawaiz.chaudhry}@estudiante.uam.es,

{juancarlos.sanmiguel, alvaro.garcia, pablo.ayuso, pablo.carballeira}@uam.es

Abstract

Pedestrian Attribute Recognition (PAR) is a challenging task as models are required to generalize across numerous attributes in real-world data. Traditional approaches focus on complex methods, yet recognition performance is often constrained by training dataset limitations, particularly the under-representation of certain attributes. In this paper, we propose a data-centric approach to improve PAR by synthetic data augmentation guided by textual descriptions. First, we define a protocol to identify weakly recognized attributes across multiple datasets. Second, we propose a prompt-driven pipeline that leverages diffusion models to generate synthetic pedestrian images while preserving the consistency of PAR datasets. Finally, we derive a strategy to seamlessly incorporate synthetic samples into training data, which considers prompt-based annotation rules and modifies the loss function. Results on popular PAR datasets demonstrate that our approach not only boosts recognition of underrepresented attributes but also improves overall model performance beyond the targeted attributes. Notably, this approach strengthens zero-shot generalization without requiring architectural changes of the model, presenting an efficient and scalable solution to improve the recognition of attributes of pedestrians in the real world.

1. Introduction

Pedestrian Attribute Recognition (PAR) aims to identify multiple soft biometric attributes of individuals in human-centric AI systems. Despite significant advances in deep learning-based approaches, achieving stable and consistent performance across all attributes remains a challenge [1]. Most state-of-the-art models struggle with imbalanced and under-represented attribute distributions derived from real-world data [2], leading to suboptimal recognition for cer-

tain attributes, even with sophisticated learning architectures. Many attributes appear infrequently or with limited variability, making it difficult for models to learn generalizable representations. Additionally, in zero-shot learning scenarios, where models must recognize attributes of people identities that were not seen during training, further expose the limitations of conventional PAR approaches.

Recently, generative AI has emerged as a solution to address data scarcity in computer vision tasks [3]. Methods based on Generative Adversarial Networks, Variational Autoencoders, and Diffusion Models (DMs) have been extensively explored for synthesizing high-quality images to support data augmentation and zero-shot learning. Among these, DMs have recently gained prominence to generate highly realistic and diverse images while providing fine-grained control over content [4]. Despite the success of DMs, their potential for augmenting PAR datasets remains relatively unexplored, presenting a promising avenue for improving attribute recognition performance.

In this paper, we propose a data-centric approach to improve PAR performance through synthetic data. Instead of increasing model complexity, we enhance data representation quality by generating synthetic pedestrian images to address the imbalance of under-represented attributes. Extensive experiments on popular datasets (RAPv1, RAPv2 [5], and RAPzs [6]) show that our method boosts recognition of augmented attributes while preserving overall robustness.

Our contributions are threefold: (1) **A systematic protocol** to identify weakly recognized attributes across multiple datasets; (2) **A prompt-driven pipeline** leveraging diffusion models to generate synthetic pedestrian images while preserving dataset consistency; and (3) **An integration strategy for PAR** data augmentation that modifies the loss function to seamlessly incorporate synthetic samples into training, ensuring smooth adaptation of new data.

2. Related Work

2.1. PAR: Methods and Datasets

Recent approaches for Pedestrian Attribute Recognition (PAR) integrate attribute-specific characteristics beyond architectural improvements [7], where ResNet is a popular backbone [6, 8, 9]. For example, discrimination can be enhanced by introducing location-aware associations of attributes with body regions [10]. Similarly, attention mechanisms [11] can be used to model attribute correlations, enabling to refine predictions. Dataset biases can also introduce inconsistencies for learning these attribute relationships, being addressed by information-theoretic regularization [12]. Multi-task transformers have been also proposed to capture global and local relations [13]. In summary, many recent approaches focus on algorithmic complexity or inter-attribute correlations to enhance PAR performance.

These complex PAR approaches rely on datasets with challenges for data distribution and generalization. For example, PETA [14] and PA100K [15] cover both indoor and outdoor environments, while RAPv1 and its extension RAPv2 [5] focus on indoor surveillance with a richer set of attributes. While efforts such as PETAZs and RAPZs [6] have aimed to address zero-shot learning, PAR datasets remain highly imbalanced, with certain attributes severely underrepresented. Consequently, models trained on them struggle to generalize, and leveraging inter-attribute relationships proves ineffective, leading to biased learning.

2.2. Text-guided Synthetic Image Generation

Generative AI has become a powerful tool to mitigate dataset biases and augment training visual data [16], with Generative Adversarial Networks (GANs) widely used to enhance data diversity. Early attempts to generate synthetic PAR data relied on unconditional GANs [17], lacking fine-grained control over individual attributes. More recently, Diffusion Models (DMs) have surpassed GANs [4], achieving high realism and diversity while allowing conditioning mechanisms, such as prompts or images. This flexibility has led to the rise of highly popular models, including DALL-E [18] and Stable Diffusion [19]. Hence, DMs arise as an option for generating PAR-like images with precise control over attributes, ensuring dataset consistency while adapting to diverse real-world scenarios.

Generating visual data through textual prompts is a powerful yet non-trivial task, especially when aiming to match the appearance of a target domain. DMs allow *text-to-image generation* (txt2img), but standard prompting can lead to inconsistent attributes, unrealistic data, or domain mismatches [20]. Therefore, *Prompt Engineering* refines prompt design to better align generated images with the target domain without modifying the model. For example, *Wildcards and Template-Based Prompts* introduce con-

trolled attribute variation ensuring dataset realism [21], while *Textual Inversion* learns custom token embeddings to generate domain-consistent data without retraining [22]. Conversely, *Model Adaptation* enhances control in txt2img diffusion. *Prompt-to-Prompt* [23] refines attributes via attention map adjustments, while LoRA fine-tuning [24] efficiently adapts models by updating a small parameter subset.

Despite PAR’s challenges with class imbalance and domain bias, these techniques remain unexplored. This paper first examines prompt engineering to ensure realistic, attribute-consistent images before model adaptation.

3. Proposed Approach

Our proposal considers three steps to enhance Pedestrian Attribute Recognition (PAR) with synthetic images. First, we *identify weakly recognized attributes* by analyzing class imbalance and recognition performance. Next, we generate *synthetic pedestrian images* using a diffusion-based pipeline, ensuring realistic attribute representations. Finally, we *integrate the synthetic data* into training by labeling the data and adapting the loss function. The next subsections outline the proposal; further details of the proposal are available in the supplementary material¹.

3.1. Identifying Weakly Recognized Attributes

We start by identifying the worst-performing attributes to apply our data-centric synthetic augmentation. Given one or more PAR training/test sets $D^j = \{(x_i^j, y_i^j), i = 1, 2, \dots, N_j\}$, where j indexes each dataset that contains N_j pedestrian images. Each image is annotated with M shared binary attributes $y_i^j \in \{0, 1\}^M$. Our goal is to determine which attributes require augmentation.

Identification Criteria: We identify weakly recognized attributes using three criteria: (1) class imbalance, (2) test-time performance, and (3) performance drop from training to testing. Attributes with few training samples are direct candidates for augmentation, while those with high test performance are deprioritized. Additionally, attributes showing a large drop in performance between training and testing indicate possible overfitting.

Criteria Scores: We employ a qualitative scoring system, assigning each attribute a score of 0 (worst case), 1 (medium), or 2 (best case). We propose a thresholding approach to define these categories, with threshold values derived from experimental analysis and insights from related work (e.g., attributes with fewer than 3% of training samples are considered underrepresented, following [6]). Table 1 summarizes the thresholds applied in this study. The final scores are obtained by adding the individual scores.

¹<http://www-vpu.eps.uam.es/AVSS2025PAR>

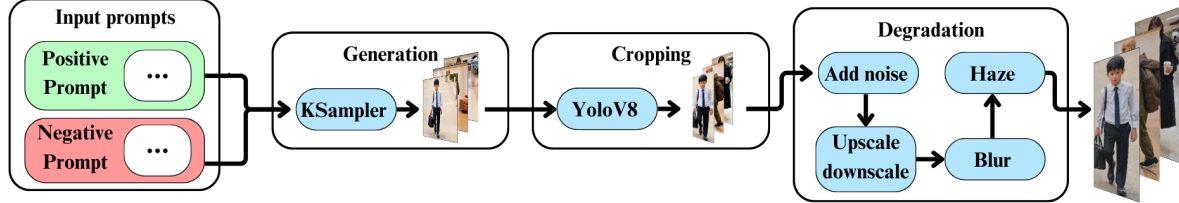


Figure 1: Proposed diffusion-based pipeline for synthetic PAR-like image generation.

Table 1: Thresholds for qualitative scoring of PAR attributes over one or multiple datasets.

Categorization (Score)	Low training images	Test performance	Drop in performance
Best (2)	False ($>3\%$)	High (>80)	Small (<15)
Medium (1)	-	Medium (50-80)	Medium (15-30)
Worst (0)	True ($<3\%$)	Low (<50)	Big (>30)

A highly detailed, ultra high definition image of a single pedestrian poses on backgrounds, with the pedestrian fully visible and centered in the frame. The pedestrian is visible from head to toe and is the primary focus, and the scene features realistic, natural colors. We have views. The subject is wearing a styles. colors. It can also be seen how the pedestrian attributes.

Figure 2: Positive prompt for PAR-like image generation.

3.2. Synthetic PAR-like Image Generation

After identifying the attributes to improve, we propose a pipeline based on text-to-image generation to ensure controlled outputs (see Figure 1), which is described as follows.

Input Prompts for Attributes: Designing effective prompts is crucial to generate diverse yet representative PAR dataset images. Our approach follows the *Wildcards and Template-Based Prompts* strategy, where wildcards are dynamically replaced with pre-configured phrases based on predefined probabilities. This allows for richer, more complex prompts that better reflect dataset characteristics. We analyzed PAR datasets to define each wildcard, resulting in the positive prompt shown in Figure 9. Additionally, negative prompts were used to exclude undesired concepts. Thus, the resulting prompts provide a richer variability and complexity (see examples in Figure 10).

Image Generation and Cropping: Diffusion models often struggle with generating tiny images [4], whereas PAR images are typically small. To ensure high-quality attribute generation, we first produce high-quality 2784×1024 resolution images, then crop them using a pedestrian detector to ensure the pedestrian remains the sole main object.

PAR-Style Image Degradation: We introduce a degradation module to match PAR image quality, which adds



Figure 3: Samples generated with the proposed prompt for each one of the pedestrian attributes.



Figure 4: Image modification as it goes through the different steps of the proposed degradation process.

noise, resizes images to simulate pixelation, applies Gaussian blur, and adjusts brightness/contrast to mimic security camera effects in PAR. An example is shown in Figure 4.

3.3. Integrating Synthetic Data into PAR Datasets

After generating images for each specific attribute, a protocol is needed to label the new images, integrate them for training, and adjust the loss function for seamless training.

Automated Data Annotation: Manually annotating synthetic images is impractical, so we modify the annotation vectors while preserving their original structure. Instead of one-hot encoding, we introduce a richer labeling scheme: -1 (uncertain presence), 1 (confirmed presence for the target attribute), and 3 (high confidence based on the prompt). The lack of 0 s (certainty of absence) aligns with dataset inconsistencies where mutually exclusive attributes are not strictly enforced. Similarly, 2 s are avoided to maintain compatibility with existing annotations, where they are later mapped to 1 s in the baseline considered [6]. The distinc-

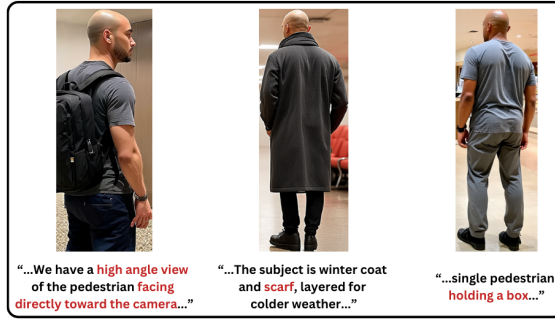


Figure 5: Generated samples with part of the prompt missing on the attributes of the image.

tion between 1 (main attribute) and 3 (other attributes) ensures that only manually verified attributes receive a 1, as prompts more reliably generate the target attribute when explicitly reinforced at the end, unlike wildcard-based attributes, which may occasionally fail (see Figure 5).

Loss Function Modification: To employ our augmented images and labels, we introduce *Binary Cross Entropy Augmented* (\mathcal{L}_{aug}), defined for each i th train image as:

$$\mathcal{L}_{aug} = -\frac{1}{M} \sum_{m=1}^M w_{i,m} \cdot \left(\mathbf{1}_{y_{i,m} \neq 0} \cdot \log \hat{y}_{i,m} + \mathbf{1}_{y_{i,m} = 0} \cdot \log(1 - \hat{y}_{i,m}) \right) \quad (1)$$

where $y_{i,m}, m \in \{0, 1\}^M$ is the (augmented or original) label for the m attribute, $\hat{y}_{i,m}$ is the predicted probability, M is the number of attributes, and $w_{i,m}$ weighs the augmented data to optimize training performance:

$$w_{i,m} = \begin{cases} 0, & \text{if } y_{i,m} = -1 \\ \text{weight_augmented}, & \text{if } y_{i,m} = 3 \\ 1, & \text{if } y_{i,m} \in \{0, 1, 2\} \end{cases}, \quad (2)$$

where attributes labeled as -1 are ignored, and those labeled as 3 contribute proportionally to *weight_augmented*.

4. Experimental Results

We begin by identifying weak attributes across selected datasets, followed by studying key hyperparameters for generating synthetic images, and training a PAR model with both real and synthetic data. Extended results with additional metrics are available in the supplementary material.

4.1. Setup

Datasets: We selected the RAP datasets (RAPv1 and RAPv2 [5], and RAPzs [6]), as they share most attributes while retaining distinct characteristics. Our study employs 152K images and 35 common attributes, providing a balanced dataset size and a strong framework for attribute analysis. We use the default train-test partitions.

Evaluation Metrics: We used the F1 Score, standard in PAR [7], as the harmonic mean of Precision and Recall.

Table 2: Performance comparison of the baseline and optimized model on the RAP datasets. Best results in bold.

PAR Approach	Hyperparams		RAPv1	RAPv2	RAPzs
	WD	BS	F1	F1	F1
Baseline [6]	$5e^{-4}$	64	79.95	78.68	77.66
Optimized	$5e^{-3}$	16	80.30	79.38	78.20

Table 3: Top-10 lowest-performing attributes in RAP datasets based on the proposed scoring methodology. Action and 'Others' attributes are excluded from this study.

Rank	RAPv1	RAPv2	RAPzs
1	hs-BaldHead	ub-Others	hs-BaldHead
2	hs-Muffler	shoes-Cloth	ub-ShortSleeve
3	ub-Tight	lb-ShortSkirt	shoes-Cloth
4	attach-PaperBag	lb-Dress	lb-ShortSkirt
5	hs-Hat	attach-HandBag	attach-PlasticBag
6	ub-SuitUp	attach-PlasticBag	attach-PaperBag
7	ub-ShortSleeve	attach-PaperBag	ub-SuitUp
8	lb-ShortSkirt	hs-BaldHead	ub-Tight
9	AgeLess16	hs-Hat	attach-Backpack
10	BodyFat	AgeLess16	AgeLess16

Implementation Details: Our generative pipeline is built on Stable Diffusion 3 implemented with ComfyUI² to handle the integration of the pipeline blocks. For training, we employed a widely used PAR architecture that combines a ResNet backbone with an MLP classifier [6, 8, 9], being trained with 256x128 images as in [6, 2]. The code implementation of our proposal is available at Github³.

4.2. Assessing the Attributes to Improve

Optimizing PAR Model Training: To ensure model robustness, we optimized weight decay (WD) and batch size (BS) while keeping other hyperparameters as in [6]: optimizer (Adam), learning rate ($1e^{-3}$) and 30 epochs. We analyzed 16 configurations by combining four WD ($5e^{-5}$ to $5e^{-2}$) and four BS (8 to 64), finding BS=16 and WD= $5e^{-3}$ to yield the best results for all datasets (see Table 2).

Attribute Ranking and Selection: Table 3 shows the lowest-ranked attributes for the proposed scores in Sec. 3.1, many of which suffer from class imbalance, ambiguity, or occlusion. Given the difficulty of replicating actions and vague attributes like 'others' using text-guided synthetic images, we focus on attributes easier to describe, and thus more reliable to synthesize. We prioritize augmentation for *hs-BaldHead*, *lb-ShortSkirt*, *AgeLess16*, *ub-SuitUp*, and *attach-PaperBag*, as they frequently appear in datasets.

²<https://github.com/comfyanonymous/ComfyUI>

³<https://github.com/vpulab/PARtxt2img>

Table 6: Attribute-level F1-score comparison for different data augmentation (DA) percentages on the RAP datasets. Best results for each dataset and attribute are in bold.** refers to our optimized model (see Table 2).

DA (%)	<i>hs-BaldHead</i>			<i>lb-ShortSkirt</i>			<i>AgeLess16</i>			<i>ub-SuitUp</i>			<i>attach-PaperBag</i>		
	RAPv1	RAPv2	RAPzs	RAPv1	RAPv2	RAPzs	RAPv1	RAPv2	RAPzs	RAPv1	RAPv2	RAPzs	RAPv1	RAPv2	RAPzs
0*	47.46	66.67	37.50	68.62	62.54	51.30	75.82	70.14	59.02	69.29	65.83	66.67	45.79	42.90	9.30
50	55.88	63.86	28.57	65.57	61.65	49.43	75.86	71.64	44.68	67.70	65.50	64.25	51.35	41.48	17.72
100	60.61	68.24	37.50	68.51	59.35	46.56	76.82	71.77	48.00	68.42	66.87	67.94	51.10	41.09	20.93
200	61.54	66.13	26.67	66.11	59.54	50.00	77.12	72.11	56.07	67.02	64.55	63.68	49.54	40.00	25.88
300	59.70	67.04	36.36	65.50	59.72	45.53	78.05	72.83	58.72	66.99	65.07	66.02	54.17	41.64	33.33
400	61.54	64.13	36.36	67.68	61.72	45.42	78.67	72.25	52.94	68.25	66.00	65.37	45.37	44.14	30.93
500	63.49	68.16	40.00	63.49	56.60	48.28	76.19	72.14	56.41	66.30	63.19	68.32	49.28	45.14	23.38

Table 4: Attribute-level F1-score comparison of noise levels for *hs-BaldHead* attribute on the RAP datasets. An augmentation weight of 0.5 was employed.

Noise level	RAPv1	RAPv2	RAPzs
Big noise (75%)	53.12	66.67	23.53
Medium noise (50%)	63.49	68.16	40.00
Small noise (25%)	58.62	66.29	40.00
Optimized from Table 2	47.46	66.67	37.50

Table 5: Attribute-level F1-score comparison of augmentation weights for *hs-BaldHead* attribute on the RAP datasets. A medium noise level was employed.

Augmentation Weight	RAPv1	RAPv2	RAPzs
0.25	61.29	65.17	14.29
0.5	63.49	68.16	40.00
0.75	53.33	64.77	40.00
1	54.24	65.90	18.18
Optimized from Table 2	47.46	66.67	37.50

4.3. Impact of Synthetic Data Augmentation

Parameter Selection for Generation: To optimize augmentation, we selected the weakest attribute *hs-BaldHead* identified in the subsection 4.2, and we evaluated two key parameters on the RAP datasets: image noise level (see Sec. 3.2) and augmented weight (see Eq. 2). By default, each real image was augmented five times, using a medium noise level and 0.5 augmentation weight. We tested three noise blending levels (25%, 50%, 75%) in Table 4, with medium noise performing best. Augmented weight, explored from 0 to 1 with four values, was optimal at 0.5 (see Table 5). These best values were used for all subsequent experiments.

Per-Attribute Performance Gains: We analyzed attribute-level F1-scores across augmentation levels (0.5–5 images per sample), ensuring consistency by using incrementally overlapping sets (e.g., 100% includes 50%). Table 6 shows that most attributes see gains as augmentation increases, confirming the effectiveness of synthetic data in enhancing PAR. Across datasets, RAPv2 benefits the most where RAPzs remains challenging, highlighting the need for further adaptation strategies in zero-shot settings.

Table 7: F1-score comparison of selected approaches for Image Data Augmentation (DA) on RAP datasets. Best, second-, and third-best results are shown in blue, green, and red, respectively. Selected DA approaches perform augmentation for all attributes available in each dataset,

whereas our proposal only focuses on the attributes *hs-BaldHead* (BH), *lb-ShortSkirt* (SK), *AgeLess16* (A16)

DA approach	BH	SK	A16	RAPv1	RAPv2	RAPzs
Proposed - 500%	✓	-	✓	80.51	79.59	78.16
Proposed - 500%	✓	✓	✓	80.60	79.67	78.62
Proposed - Best %	✓	-	✓	80.38	79.77	78.26
Proposed - Best %	✓	✓	✓	80.50	79.76	78.52
Horizont. Flip [6]	-	-	-	79.95	78.68	77.66
GANs [17]	-	-	-	77.83	-	-
AutoAug [25]	-	-	-	80.39	79.54	78.25
MixUp [26]	-	-	-	80.35	80.11	77.57
RandAug [27]	-	-	-	80.26	79.72	77.34
TrivAug [28]	-	-	-	80.55	79.64	77.46
AugMix [29]	-	-	-	80.42	79.44	77.19

While 500% provides the best F1-score in RAPv1 for *hs-BaldHead*, other attributes (e.g., *lb-ShortSkirt*, *attach-PaperBag*) do not consistently improve with extreme augmentation, indicating potential overfitting.

Overall Performance: After optimizing augmentation per attribute, we tested simultaneous augmentation across datasets. We evaluated two models: one using 500% augmentation for all attributes and another applying each attribute’s optimal augmentation level. Since *lb-ShortSkirt* showed no improvement, we also tested augmentation with only *hs-BaldHead* and *AgeLess16*. Table 7 compares state-of-the-art image augmentation methods, averaging results over 10 runs using the same architecture from [6]. It can be seen that our approach improves overall performance by augmenting 2–3 of 52 attributes, as compared to the baseline (i.e., Horizontal Flip [6]). Our method performs best on RAPv1 and RAPzs, ranking among the top 2 across all datasets and highlighting its robustness for the datasets considered. Interestingly, including *lb-ShortSkirt* often yielded the best or highly competitive results, suggesting an indirect boost to other attributes.

5. Conclusions and Future Work

This work introduced a data-centric approach for improving Pedestrian Attribute Recognition by augmenting training data with synthetic images generated by diffusion models. Instead of increasing model complexity, we identified weakly recognized attributes and selectively enhanced their representation. Experimental results demonstrated consistent improvements in attribute recognition, particularly for underrepresented ones, while maintaining overall model robustness. Notably, our method achieved comparable or superior results to more complex strategies, highlighting the effectiveness of targeted synthetic augmentation.

Future work will extend our proposal to more attributes, architectures, and datasets while exploring methods for automatically estimating the optimal augmentation size.

Acknowledgments

This work has been partially supported by the Spanish Government (PID2021-125051OB-I00) and is part of preliminary work in project TEC-2024/COM-322 (IDEALCV-CM) funded by the Regional Government of Madrid. The authors would also like to thank the anonymous reviewers for the valuable feedback provided.

References

- [1] J. Jin *et al.*, “Pedestrian attribute recognition: A new benchmark dataset and a large language model augmented framework,” *arXiv:2408.09720*, 2024.
- [2] Y. Zhou *et al.*, “Heterogeneous feature re-sampling for balanced pedestrian attribute recognition,” *IEEE Trans. Pattern Analysis and Machine Intelligence*, 2025.
- [3] Y. Chen *et al.*, “A comprehensive survey for generative data augmentation,” *Neurocomputing*, p. 128167, 2024.
- [4] F.-A. Croitoru *et al.*, “Diffusion models in vision: A survey,” *IEEE Trans. Pattern Analysis and Machine Intelligence*, vol. 45, no. 9, pp. 10 850–10 869, 2023.
- [5] D. Li *et al.*, “A richly annotated pedestrian dataset for person retrieval in real surveillance scenarios,” *IEEE Trans. Image Processing*, vol. 28, no. 4, pp. 1575–1590, 2018.
- [6] J. Jia *et al.*, “Rethinking of pedestrian attribute recognition: A reliable evaluation under zero-shot pedestrian identity setting,” *arXiv:2107.03576*, 2021.
- [7] X. Wang *et al.*, “Pedestrian attribute recognition: A survey,” *Pattern Recognition*, vol. 121, p. 108220, 2022.
- [8] N. Kirillova *et al.*, “A visual surveillance system to observe realistic road user behavior for improved pedestrian and cyclist safety at crossroads,” in *IEEE Int. Conf. Adv. Video and Signal-based Surveillance*, 2022, pp. 1–8.
- [9] H. Galiyawala *et al.*, “Discrete soft biometric attribute-based person retrieval in surveillance videos,” in *IEEE Int. Conf. Adv. Video and Signal-based Surveillance*, 2021, pp. 1–7.
- [10] J. Shen *et al.*, “SSPNet: Scale and spatial priors guided generalizable and interpretable pedestrian attribute recognition,” *Pattern Recognition*, vol. 148, p. 110194, 2024.
- [11] D. Weng *et al.*, “Exploring attribute localization and correlation for pedestrian attribute recognition,” *Neurocomputing*, vol. 531, pp. 140–150, 2023.
- [12] Y. Zhou *et al.*, “A solution to co-occurrence bias: Attributes disentanglement via mutual information minimization for pedestrian attribute recognition,” in *Int. Joint Conf. Artificial Intelligence*, 2023, pp. 1831–1839.
- [13] X. Fan *et al.*, “Transformer-based multi-task network for pedestrian attribute recognition,” *IEEE Trans. Circuits and Systems for Video Tech.*, vol. 34, no. 1, pp. 411–423, 2023.
- [14] Deng *et al.*, “Pedestrian attribute recognition at far distance,” in *ACM Int. Conf. Multimedia*, 2014, pp. 789–792.
- [15] Liu *et al.*, “Attentive deep features for pedestrian analysis,” in *IEEE Int. Conf. on Computer Vision*, 2017, pp. 350–359.
- [16] L. Lin *et al.*, “Robust clip-based detector for exposing diffusion model-generated images,” in *IEEE Int. Conf. Advanced Video and Signal-based Surveillance*, 2024, pp. 1–7.
- [17] M. Fabbri *et al.*, “Generative adversarial models for people attribute recognition in surveillance,” in *IEEE Int. Conf. Adv. Video and Signal-based Surveillance*, 2017, pp. 1–6.
- [18] A. Ramesh *et al.*, “Zero-shot text-to-image generation,” in *Int. Conf. Machine Learning*, 2021, pp. 8821–8831.
- [19] R. Rombach *et al.*, “High-resolution image synthesis with latent diffusion models,” in *IEEE/CVF Conf. Computer Vision and Pattern Recognition*, 2022, pp. 10 684–10 695.
- [20] S. Schulhoff *et al.*, “The prompt report: A systematic survey of prompting techniques,” *arXiv:2406.06608*, 2024.
- [21] W. Mo *et al.*, “Dynamic prompt optimizing for text-to-image generation,” in *IEEE/CVF Conf. Computer Vision and Pattern Recognition*, 2024, pp. 26 627–26 636.
- [22] R. Gal *et al.*, “An image is worth one word: Personalizing text-to-image generation using textual inversion,” in *Int. Conf. Learning Represen.*, 2023.
- [23] A. Hertz *et al.*, “Prompt-to-prompt image editing with cross attention control,” in *Int. Conf. Learning Represen.*, 2023.
- [24] E. J. Hu *et al.*, “Lora: Low-rank adaptation of large language models,” in *Int. Conf. Learning Represen.*, 2022.
- [25] E. D. Cubuk *et al.*, “Autoaugment: Learning augmentation strategies from data,” in *IEEE/CVF Conf. Computer Vision and Pattern Recog.*, 2019, pp. 113–123.
- [26] H. Zhang *et al.*, “mixup: Beyond empirical risk minimization,” *arXiv preprint arXiv:1710.09412*, 2017.
- [27] E. Cubuk *et al.*, “Practical automated data augmentation with a reduced search space,” in *IEEE/CVF Conf. on Computer Vision and Pattern Recognition Work.*, 2020, pp. 702–703.
- [28] S. G. Müller and F. Hutter, “Trivialaugment: Tuning-free yet state-of-the-art data augmentation,” in *IEEE/CVF Int. Conf. on Computer Vision*, 2021, pp. 774–782.
- [29] D. Hendrycks *et al.*, “Augmix: A simple data processing method to improve robustness and uncertainty,” in *Int. Conf. Learning Represen.*, 2020.

SUPPLEMENTARY MATERIAL

This supplementary material offers additional details on the prompt definition of our proposal in Section A. Moreover, we present extended information for the experiments of the paper regarding the baseline optimization (Section B), attributes analysis and ranking for the chosen datasets (Section C), and synthetic data augmentation and training (Section D). Finally, we provide configuration details for the ComfyUI tool employed for experimentation in Section E.

A. Input Prompts for Synthetic PAR-like Image Generation with attribute variation

After identifying the attributes to improve, our pipeline based on text-to-image generation generates synthetic images based on prompts. Here we provide an extended description of prompts employed.

A.1. Prompt structure

Designing an effective prompt is critical for obtaining robust results that accurately reflect the underlying dataset while providing sufficient variability to avoid overfitting to specific characteristics. In our work, the generation process must produce images resembling those in the RAP datasets, specifically depicting pedestrians cropped within airport environments and performing diverse actions as captured by security cameras. This inherently results in samples with low image quality. Examples from the original dataset are shown in Figure 6.

It is important to note, however, that upon examining the dataset, it is not difficult to find examples where the labels are incorrectly assigned (Figure 7). In our case, the goal is to align with the dataset while avoiding the introduction of noise. For *hs-BaldHead*, at least part of the scalp must be visible; for *lb-ShortSkirt*, the garment must be open between the legs and end between the waist and the knee; and for *AgeLess16*, the pedestrian must appear to fall within the indicated age range.

In our preliminary experiments, generating images with content similar to the target dataset was relatively straightforward using varied prompts. However, replicating the exact image quality proved challenging when relying solely on prompt-based generation. For instance, including descriptors such as “security camera” often led the model to produce images that deviated from the target dataset in terms of tonal distribution, watermark artifacts, noise patterns, and even fisheye distortions (see Figure 8). Furthermore, the use of negative prompts did not sufficiently alleviate these discrepancies.

As a result, we first generate high-definition images (leveraging the model’s superior performance in this task) and subsequently adjust their visual characteristics to align with the target dataset. Even taking advantage of not restraining quality by

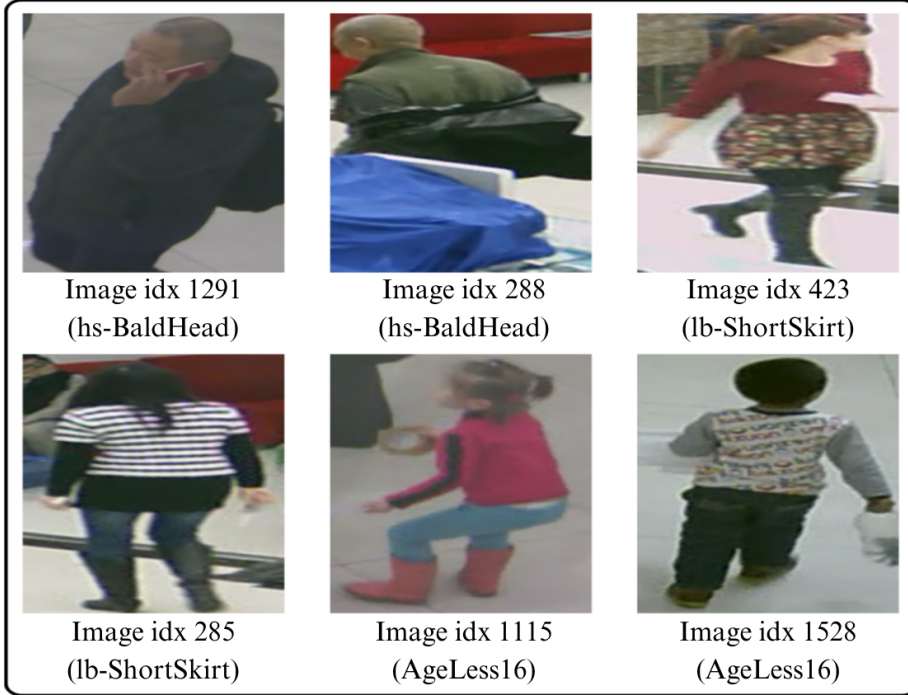


Figure 6: Dataset ground-truth samples

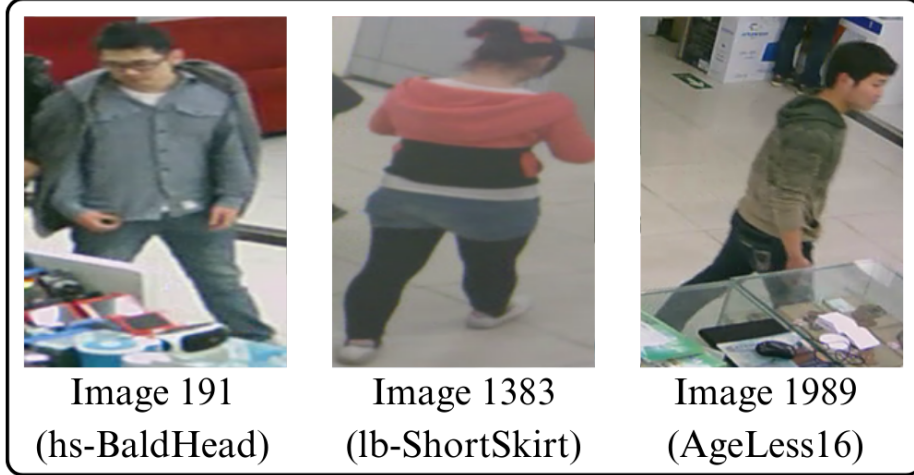


Figure 7: Noisy dataset ground-truth samples



Figure 8: Samples generated with the given prompt using keywords such as "security camera"

prompting, and although diffusion models excel generating images with considerable variability, a static prompt is inadequate to capture the full spectrum of variations inherent in the dataset.

To address this limitation, our approach follows the *Wildcards and Template-Based Prompts* strategy, where wildcards are dynamically replaced with pre-configured phrases based on predefined probabilities. This allows for richer, more complex prompts that better reflect dataset characteristics. We analyzed PAR datasets to define each wildcard, resulting in the positive prompt shown in Figure 9. Additionally, negative prompts were used to exclude undesired concepts. Thus, the resulting prompts provide a richer variability and complexity (see examples in Figure 10).

A highly detailed, ultra high definition image of a single pedestrian `poses` on `backgrounds`, with the pedestrian fully visible and centered in the frame. The pedestrian is visible from head to toe and is the primary focus, and the scene features realistic, natural colors. We have `views`. The subject is wearing a `styles`. `colors`. It can also be seen how the pedestrian `attributes`.

Figure 9: Positive prompt for PAR-like image generation.

A.2. Wildcard definition

To characterize each wildcard, we performed a comprehensive analysis of the dataset to accurately mirror its inherent conditions. In the following, we detail the definition of each wildcard and provide representative examples. These examples, documented in Subsection A.3, are uniformly applied during practical implementation.

- **Poses:** To prevent pedestrians from consistently appearing in a walking stance, "poses" refer to diverse postures (e.g.,



Figure 10: Samples generated with the proposed prompt for each one of the pedestrian attributes.

“crossing arms while standing”, “moving with hands behind the back”) or subtle actions (e.g., “using a smartphone”, “holding paper or documents”) observed directly in the dataset.

- **Backgrounds:** Although all images are set in airport interiors, the backgrounds vary. Based on observed examples, wildcards such as “an airport terminal waiting area” or “an indoor shopping center walkway” are introduced. Some descriptions, despite not explicitly mentioning the airport, mimic backgrounds present in the dataset.
- **Views:** Views adjust the visible portion of the pedestrian to enhance generalization. Examples include “a clear view of the back of the person, captured from behind” or “a high-angle view of the profile of the pedestrian”, replicating typical security camera angles.
- **Styles:** In generating images for the bald-head attribute, we observed that the model tended to depict bald individuals wearing either suits or gym attire when representing people of color. To introduce variability, clothing styles such as “casual t-shirt and jeans” or “winter coat and scarf, layered for colder weather” were incorporated.
- **Colors:** This wildcard pertains to the color scheme of the previously mentioned clothing styles. Examples include descriptions like “practical and functional colors, with dark tones such as black, grey, and navy” or “vibrant, eye-catching colors, including bright reds, oranges, and yellows.”
- **Attributes:** This wildcard, expressed in a separate sentence from the others, specifically addresses the augmented attribute. To ensure consistency with the dataset, the term “asian” is incorporated, yielding examples such as “is a bald Asian person”, “is an Asian person wearing a short skirt with tights or leggings”, and “is an Asian kid or teenager clearly not older than 15 years old.”

A.3. Prompt definition

The prompts used for image generation are described below, including both positive and negative prompts, as well as the wildcards employed. The objective is to document exactly how each image could have been generated.

First, the negative prompt used to guide the generation was:

"bad quality, poor quality, Partial figures, cropped bodies, cut-off limbs, headless or footless pedestrians, close-up shots, extreme zoom, obscured views, hidden or partially visible subjects, cropped at the knees or waist, off-frame figures, incomplete visibility, overly zoomed-in perspectives"

This aims, in general, to produce images of the highest possible quality where a pedestrian is clearly visible as the main element of the image. Additionally, for the generation of *shortskirts*, the following was appended to the prompt to avoid generations resembling short skirts that do not meet the defined criteria:

", no pants, no long skirts, no oversized clothing."

Regarding the positive prompt, the one used is as mentioned in the corresponding section of the report, specifically:

"A highly detailed, ultra high definition image of a single pedestrian _poses_ on _backgrounds_, with the pedestrian fully visible and centered in the frame. The pedestrian is visible from head to toe and is the primary focus, and the scene features realistic, natural colors. We have _views_. The subject is wearing a _styles_. _colors_. It can also be seen how the pedestrian _attributes_."

As for the wildcards and their intended purposes, below are the specific values they can contain:

attributes: (*One of these is selected based on the attribute being augmented*)

- is a bald asian person
- is an asian person wearing a short skirt with tights or leggings
- is an asian kid or teenager clearly not older than 15 years old
- is a female asian child

backgrounds:

- a shopping mall interior with glass storefronts
- a shopping center walkway
- an indoor shopping mall food court
- an indoor escalator near shops
- an indoor walkway near escalators
- an indoor office building corridor
- an office lobby with elevators
- an indoor public lobby with seating
- an airport terminal waiting area
- an airport security checkpoint

colors:

- The outfit is vibrant and full of bold, eye-catching colors, such as bright reds, oranges, and yellows.
- The look incorporates a balanced mix of soft and bright tones, like pastel pinks, light blues, and subtle greens, creating a modern, trendy appearance.
- The style is composed of subtle, muted shades with minimal color contrast, such as grey, beige, and light brown, blending naturally into the background.
- The outfit follows a monochromatic palette, staying within a single color family, like different shades of black, white, or navy, giving the pedestrian a sleek, cohesive look.
- The style features natural, earthy hues that create a calm, understated appearance, with tones like olive green, brown, and khaki.
- The colors are practical and functional, with dark tones like black, grey, and navy.
- The outfit contrasts between dark and light elements, with bright whites or light greys paired with deep blues or blacks, creating a visually striking yet balanced style.
- The pedestrian's clothing includes soft neutral tones like beige, off-white, and light grey, creating a subtle, relaxed appearance.

- The outfit incorporates rich, formal colors like maroon, charcoal grey, and dark green.
- The style is colorful yet refined, using contrasting accents like a red accessory paired with a neutral-toned outfit, drawing attention while maintaining sophistication.

—poses—:

- walking
- standing still
- using a smartphone
- holding a shopping bag
- carrying a backpack
- carrying a shoulder bag
- carrying a small bag in the front
- carrying a small bag on the side
- holding a shopping bag with both hands
- with their hands in the pockets
- crossing arms while standing
- adjusting clothing
- looking to the side
- looking down at a phone
- walking while holding a coffee cup#(action-Holding)
- standing with one hand on hip
- holding a jacket
- carrying a jacket over the shoulder
- holding a water bottle
- carrying multiple items in hand
- moving with hands behind the back
- holding paper or documents
- holding a box
- checking or exploring a box
- carrying a box
- moving a big box or large items
- carrying multiple bags

—styles—:

- casual t-shirt and jeans
- formal business suit with a tie
- business casual outfit with a button-up shirt and slacks
- jacket over a t-shirt with jeans
- hoodie and sweatpants
- sporty outfit with a windbreaker and jogging pants
- leather jacket, streetwear style and jeans, streetwear style

- long overcoat over a sweater and slacks
- short-sleeved shirt with chinos
- winter coat and scarf, layered for colder weather
- light jacket, appropriate for indoor walking and jeans, appropriate for indoor walking
- blazer with a button-up shirt and chinos
- polo shirt, semi-casual look with khaki pants, semi-casual look
- denim jacket with a t-shirt and sneakers
- sweater over a collared shirt with dress pants
- windbreaker, outdoor casual style and jeans, outdoor casual style
- puffer jacket, typical for colder weather with casual pants, typical for colder weather
- cardigan over a long-sleeve shirt and jeans

In the case of generating shortskirts, all attributes related to pants have been excluded, leaving the following:

- casual t-shirt
- formal business suit with a tie
- business casual outfit with a button-up shirt
- jacket over a t-shirt
- hoodie
- casual dress or skirt with a jacket
- sporty outfit with a windbreaker
- leather jacket, streetwear style
- long overcoat over a sweater
- short-sleeved shirt
- winter coat and scarf, layered for colder weather
- light jacket, appropriate for indoor walking
- blazer with a button-up shirt
- polo shirt, semi-casual look
- denim jacket with a t-shirt and sneakers
- summer dress with sandals
- sweater over a collared shirt
- windbreaker, outdoor casual style
- puffer jacket, typical for colder weather
- cardigan over a long-sleeve shirt

__views__:

- a clear front view of the subject, facing directly toward the camera
- a complete side view of the subject, captured in profile
- a clear view of the back of the person, captured from behind
- a high angle view of the pedestrian facing directly toward the camera
- a high angle view of the profile of the pedestrian
- a high angle view of the back of the pedestrian, as the image is captured from behind

Table 8: Performance metrics for different weight decay values (RAPv1).

Weight decay	ma	Acc	Prec	Rec	F1
5e-2	68.77	65.03	80.87	75.16	77.91
5e-3	78.14	68.97	81.2	80.13	80.48
5e-4	79.76	68.47	80.11	80.46	80.29
5e-5	78.71	67.82	80.15	79.52	79.84
5e-4 (theirs)	79.27	67.98	80.19	79.71	79.95

Table 9: Performance metrics for different batch sizes (RAPv1).

Batch size	ma	Acc	Prec	Rec	F1
8	80.86	68.36	79.32	81.22	80.26
16	80.78	68.68	79.98	80.99	80.66
32	79.76	68.47	80.11	80.46	80.29
64	78.88	67.94	80.18	79.59	79.88
64 (theirs)	79.27	67.98	80.19	79.71	79.95

Table 10: Performance metrics comparison with best batch size, weight decay and combination (RAPv1).

Modification	ma	Acc	Prec	Rec	F1
WD 5e-3	78.14	68.97	81.2	80.13	80.48
BS 16	80.78	68.68	79.98	80.99	80.66
BS 16 + WD 5e-3	71.94	66.63	80.78	77.42	79.06
Base model (theirs)	79.27	67.98	80.19	79.71	79.95

Table 11: Performance metrics comparison between base and optimized model (RAPv1)

Metric	ma	Acc	Prec	Rec	F1
Base performance	79.27	67.98	80.19	79.71	79.95
Performance optimized model	80.54	68.49	79.89	80.72	80.30

B. Extended experimental results for optimizing PAR Model Training

The architecture and training employed follows the general structure provided by Jia et al. [6]. However, to ensure that the attribute analysis is as meaningful as possible, the model has undergone a hyperparameter optimization per dataset before obtaining the baseline results, so that the model analyzed has achieved the best performance.

Optimization for RAPv1: The optimization process commenced with RAPv1, the smallest subset within the RAP datasets. For efficiency, a set of relevant hyperparameters was selected to tune using a one-dimensional grid search, addressing each parameter individually. More complex search strategies were discarded due to the large number of hyperparameters involved.

The chosen hyperparameters were those that significantly influenced the model’s performance or that differed with the baseline [6] and the latest GitHub implementation. Based on these criteria, the final set included batch size, classifier, learning rate, optimizer, and weight decay. Tables 8 and 9 summarize the parameters that, when adjusted, led to superior performance compared to the baseline reported by the original authors.

As shown in Table 10, we improved the overall results by individually modifying weight decay and batch size. Based on these findings, we evaluated a combined configuration of the best-performing settings for both parameters. However, jointly modifying the parameters yielded inferior results, leading us to adjust only the batch size, reducing it to 16. The final model was executed multiple times to ensure robust performance, and the final optimized results on RAP1 are reported in Table 11.

Optimization for RAPv2: Observing the results for RAPv1, and noting the potential influence of batch size on the optimal settings for other hyperparameters, we extended the previous strategy by incorporating combinations of batch size with each hyperparameter. If any combination yielded improved performance, we proposed to replicate the experiments on RAPv1.

Table 12: Performance metrics for different weight decays and batch sizes combinations (RAPv2).

Weight Decay	Batch Size	ma	Acc	Prec	Rec	F1
5e-3	16	71.73	65.55	79.31	77.43	78.36
5e-3	32	75.11	67.12	79.57	79.3	79.43
5e-3	64	76.24	67.84	80.01	79.76	79.89
5e-4	16	79.06	67.18	78.38	80.43	79.39
5e-4	32	78.81	67.07	78.51	80.07	79.28
5e-4	64	77.89	66.73	78.7	79.36	79.03
5e-5	16	79.38	66.84	77.89	80.43	79.14
5e-5	32	78.68	66.71	78.17	79.95	79.05
5e-5	64	78.15	66.82	78.58	79.63	79.1
5e-4 (theirs)	64 (theirs)	78.52	66.09	77.2	80.23	78.68

Table 13: Performance metrics comparison between base and optimized model (RAPv2).

Performance	ma	Acc	Prec	Rec	F1
Base model	78.52	66.09	77.2	80.23	78.68
Optimized model	79.12 ± 0.1021	67.17 ± 0.1037	78.35 ± 0.0874	80.43 ± 0.1175	79.38 ± 0.0869

Table 14: Performance metrics for different batch sizes (RAPzs).

Batch size	ma	Acc	Prec	Rec	F1
8	74.07	65.53	78.03	78.22	78.13
16	73.18	65.84	79.01	77.69	78.35
32	72.2	65.05	78.81	76.82	77.8
64	71.76	64.83	78.75	76.6	77.66
64 (theirs)	71.18	64.54	78.85	76.02	77.41

Table 15: Performance metrics comparison between base and optimized model (RAPzs).

Performance	ma	Acc	Prec	Rec	F1
Base	71.76	64.83	78.75	76.6	77.66
Optimized model	74.39 ± 0.2155	65.59 ± 0.2281	78.19 ± 0.1459	78.20 ± 0.2664	78.20 ± 0.1868

The set of hyperparameters remained unchanged, with the addition of using an EMA model, and the performance improvements were comparable. Notably, modifying only the batch size and weight decay yielded superior results relative to the base model. Table 12 illustrates the joint optimization of these parameters, where a batch size of 16 produced the best overall performance. Although a weight decay of 5e-3 with a batch size of 64 achieved more peak values, the batch size of 16 consistently enhanced all metrics and showed greater stability. The final optimized parameters are listed in Table 13.

Optimization for RAPzs: In the case of RAPzs, after evaluating the trend in the other datasets of the same family, it was decided to focus the optimization process on the batch size. As can be seen in table 14, in this case, even smaller values than those being used in the other datasets continue to improve the results, but it was decided to stop at 8 to avoid having too small a batch size that could slow down the training process. The final results are in Table 15.

C. Extended experimental results for Attribute analysis

Here, we provided further details on the attribute performance (see subsection C.2), the assigned scores using the proposed approach (see subsection C.2), and the identified critical attributes for each dataset (see Subsection C.3) and globally (see Subsection C.4). These identified attributes are the best candidates to be improved by using synthetic data.

C.1. Attribute performance per dataset

The following Tables provide performance results for Train and Test sets of RAPv1, RAPv2 and RAPzs. We employ all common metrics to measure PAR performance (ma, Acc, Prec, Rec and F1).

Table 16: RAPv1 training results per attribute

Attribute Number	Attribute Name	ma	Acc	Prec	Rec	F1	Num images
1	hs-BaldHead	87.28	69.47	91.00	74.59	81.98	122
2	hs-LongHair	97.27	88.94	91.85	96.57	94.15	6348
3	hs-BlackHair	92.41	98.32	99.17	99.14	99.15	31437
4	hs-Hat	96.41	89.07	95.58	92.90	94.22	535
5	hs-Glasses	94.86	79.31	86.16	90.89	88.46	2459
6	hs-Muffler	83.43	57.49	80.13	67.04	73.01	355
7	ub-Shirt	96.04	87.72	92.75	94.17	93.46	7340
8	ub-Sweater	87.13	60.24	72.05	78.61	75.18	4151
9	ub-Vest	97.87	92.84	96.64	95.94	96.29	1920
10	ub-TShirt	89.48	70.35	80.21	85.13	82.60	7557
11	ub-Cotton	95.07	83.90	90.27	92.24	91.25	5817
12	ub-Jacket	94.34	84.62	89.86	93.55	91.67	10496
13	ub-SuitUp	92.68	76.82	88.20	85.61	86.89	716
14	ub-Tight	92.11	76.38	88.78	84.54	86.61	983
15	ub-ShortSleeve	94.61	84.18	93.59	89.34	91.41	572
16	lb-LongTrousers	96.08	93.15	97.08	95.84	96.45	18660
17	lb-Skirt	98.58	91.27	93.32	97.65	95.44	2174
18	lb-ShortSkirt	94.86	78.66	86.07	90.13	88.06	912
19	lb-Dress	96.85	86.11	91.06	94.06	92.54	1246
20	lb-Jeans	97.14	91.27	94.59	96.30	95.44	8893
21	lb-TightTrousers	97.43	87.58	90.54	96.41	93.38	4456
22	shoes-Leather	92.39	79.87	86.96	90.74	88.81	10119
23	shoes-Sport	87.05	65.81	74.74	84.63	79.38	8957
24	shoes-Boots	97.73	90.48	93.65	96.40	95.00	4162
25	shoes-Cloth	84.65	48.09	60.67	69.88	64.95	415
26	shoes-Casual	78.21	45.60	61.50	63.82	62.64	5202
27	attach-Backpack	94.42	83.01	92.52	88.98	90.72	626
28	attach-SingleShoulderBag	95.75	85.10	91.86	92.04	91.95	2100
29	attach-HandBag	94.05	80.34	89.81	88.40	89.10	957
30	attach-Box	94.34	79.29	87.68	89.24	88.45	1404
31	attach-PlasticBag	91.33	72.59	85.18	83.08	84.12	934
32	attach-PaperBag	86.01	58.69	75.73	72.29	73.97	397
33	attach-HandTrunk	98.40	89.24	91.76	97.01	94.32	804
34	attach-Other	91.10	77.75	87.60	87.37	87.48	9809
35	AgeLess16	94.45	86.59	97.06	88.92	92.81	334
36	Age17-30	89.63	78.82	87.30	89.03	88.16	14296
37	Age31-45	89.70	83.12	91.47	90.10	90.78	18638
38	Female	98.64	96.45	98.42	97.97	98.19	10213
39	BodyFat	86.14	60.96	74.91	76.59	75.74	4781
40	BodyNormal	81.00	83.77	89.69	92.70	91.17	24695
41	BodyThin	81.93	52.63	71.27	66.81	68.97	3290
42	Customer	94.97	99.09	99.44	99.64	99.54	31454
43	Clerk	98.97	93.17	94.78	98.22	96.47	1626
44	action-Calling	97.45	89.98	94.35	95.10	94.72	1142
45	action-Talking	66.78	27.24	56.52	34.46	42.82	1094
46	action-Gathering	75.07	40.51	62.77	53.33	57.66	3051
47	action-Holding	86.25	62.23	80.92	72.93	76.72	820
48	action-Pushing	90.84	68.97	81.40	81.87	81.63	342
49	action-Pulling	93.31	75.00	84.56	86.90	85.71	580
50	action-CarrybyArm	90.12	72.18	87.45	80.53	83.85	796
51	action-CarrybyHand	94.99	81.13	87.34	91.94	89.58	4271
Avg		91.52	84.56	90.63	91.77	91.20	

Table 17: RAPv1 test results per attribute

Attribute Number	Attribute Name	ma	Acc	Prec	Rec	F1	Num images
1	hs-BaldHead	69.39	31.11	60.87	38.89	47.46	36
2	hs-LongHair	93.44	78.83	86.31	90.10	88.16	1525
3	hs-BlackHair	83.86	96.45	98.19	98.19	98.19	7851
4	hs-Hat	85.77	61.17	80.42	71.88	75.91	160
5	hs-Glasses	88.69	64.08	77.12	79.13	78.11	575
6	hs-Muffler	70.28	24.09	36.67	41.25	38.82	80
7	ub-Shirt	88.21	68.65	80.81	82.02	81.41	1858
8	ub-Sweater	70.36	29.89	43.01	49.49	46.02	982
9	ub-Vest	90.71	75.00	89.80	81.99	85.71	483
10	ub-TShirt	76.56	47.08	63.46	64.59	64.02	1960
11	ub-Cotton	83.74	54.20	66.09	75.07	70.29	1368
12	ub-Jacket	82.20	60.17	72.58	77.86	75.13	2611
13	ub-SuitUp	81.92	53.01	75.00	64.39	69.29	205
14	ub-Tight	71.95	33.33	56.05	45.13	50.00	277
15	ub-ShortSleeve	82.21	56.70	82.09	64.71	72.37	170
16	lb-LongTrousers	88.87	82.23	89.91	90.59	90.25	4642
17	lb-Skirt	89.36	67.67	81.49	79.96	80.72	534
18	lb-ShortSkirt	82.16	52.23	72.57	65.08	68.62	252
19	lb-Dress	86.54	58.24	73.21	74.01	73.61	277
20	lb-Jeans	91.11	76.98	86.78	87.20	86.99	2266
21	lb-TightTrousers	91.54	72.78	82.79	85.75	84.24	1088
22	shoes-Leather	86.51	66.34	75.49	84.55	79.76	2459
23	shoes-Sport	76.06	48.74	66.41	64.69	65.54	2308
24	shoes-Boots	94.75	79.93	86.36	91.47	88.85	997
25	shoes-Cloth	82.52	43.23	55.83	65.69	60.36	102
26	shoes-Casual	68.59	29.67	41.50	51.01	45.77	1341
27	attach-Backpack	84.84	50.28	63.83	70.31	66.91	128
28	attach-SingleShoulderBag	84.88	55.72	71.25	71.88	71.57	569
29	attach-HandBag	81.27	44.26	59.21	63.68	61.36	212
30	attach-Box	78.74	45.66	67.21	58.74	62.69	349
31	attach-PlasticBag	78.47	41.14	58.57	58.02	58.29	212
32	attach-PaperBag	68.77	29.70	57.65	37.98	45.79	129
33	attach-HandTrunk	87.13	60.53	75.94	74.88	75.41	215
34	attach-Other	78.97	54.23	70.54	70.11	70.32	2442
35	AgeLess16	85.72	61.05	80.56	71.60	75.82	81
36	Age17-30	72.72	52.80	68.54	69.69	69.11	3586
37	Age31-45	73.55	61.76	77.05	75.68	76.36	4650
38	Female	96.81	91.75	96.15	95.26	95.70	2488
39	BodyFat	64.81	26.52	50.57	35.79	41.92	1246
40	BodyNormal	60.02	71.56	78.91	88.48	83.42	6181
41	BodyThin	60.40	17.16	33.17	26.23	29.29	774
42	Customer	91.24	98.32	99.11	99.19	99.15	7898
43	Clerk	94.96	79.72	86.93	90.58	88.72	382
44	action-Calling	89.50	66.07	79.42	79.71	79.57	276
45	action-Talking	55.46	8.82	24.09	12.22	16.22	270
46	action-Gathering	62.93	21.23	41.85	30.12	35.03	767
47	action-Holding	67.42	25.62	47.37	35.82	40.79	201
48	action-Pushing	87.56	53.97	65.38	75.56	70.10	90
49	action-Pulling	76.98	40.69	61.48	54.61	57.84	152
50	action-CarrybyArm	65.77	23.29	45.31	32.40	37.79	179
51	action-CarrybyHand	85.11	60.41	77.24	73.49	75.32	1090
Avg		80.22	68.61	79.98	80.75	80.36	

Table 18: RAPv2 training results per attribute

Attribute Number	Attribute Name	ma	Acc	Prec	Rec	F1	Num images
1	hs-BaldHead	90.93	76.61	92.23	81.90	86.76	116
2	hs-LongHair	96.66	87.76	91.60	95.45	93.48	4239
3	hs-BlackHair	90.05	98.28	99.08	99.18	99.13	20708
4	hs-Hat	94.39	84.29	94.27	88.85	91.48	296
5	hs-Glasses	93.07	76.10	85.71	87.16	86.43	1426
6	ub-Shirt	95.47	86.70	92.23	93.53	92.88	5384
7	ub-Sweater	82.57	52.31	67.25	70.20	68.69	2802
8	ub-Vest	97.51	92.00	96.43	95.25	95.83	1304
9	ub-TShirt	87.68	67.40	77.90	83.32	80.52	5475
10	ub-Cotton	93.40	78.47	86.96	88.94	87.94	2992
11	ub-Jacket	93.13	79.97	86.27	91.63	88.87	5846
12	ub-SuitUp	92.70	75.96	87.00	85.68	86.34	461
13	ub-Tight	88.94	68.85	85.04	78.34	81.55	711
14	ub-ShortSleeve	92.57	77.55	89.45	85.35	87.35	437
15	ub-Others	50.00	0.00	0.00	0.00	0.00	35
16	lb-LongTrousers	95.20	91.73	96.07	95.31	95.69	12110
17	lb-Skirt	94.91	80.00	87.59	90.23	88.89	665
18	lb-ShortSkirt	95.20	79.56	86.52	90.82	88.62	643
19	lb-Dress	95.37	79.34	85.71	91.43	88.48	946
20	lb-Jeans	96.38	89.17	93.35	95.21	94.28	5770
21	lb-TightTrousers	96.69	86.16	90.23	95.03	92.57	3022
22	shoes-Leather	91.26	76.55	84.50	89.05	86.72	6207
23	shoes-Sports	84.85	61.87	70.87	82.96	76.44	6075
24	shoes-Boots	97.43	89.28	92.82	95.90	94.34	2683
25	shoes-Cloth	87.93	52.14	61.95	76.70	68.54	382
26	shoes-Casual	71.81	36.18	54.92	51.46	53.13	3397
27	shoes-Other	50.00	0.00	0.00	0.00	0.00	7
28	attachment-Backpack	90.10	74.71	91.46	80.31	85.52	320
29	attachment-ShoulderBag	93.72	80.54	90.49	87.98	89.22	1190
30	attachment-HandBag	89.01	64.58	78.48	78.48	78.48	461
31	attachment-Box	90.40	70.06	83.37	81.44	82.40	820
32	attachment-PlasticBag	87.33	60.68	75.72	75.34	75.53	593
33	attachment-PaperBag	62.54	19.01	43.10	25.38	31.95	197
34	attachment-HandTrunk	96.00	82.45	88.47	92.38	90.38	656
35	attachment-Other	87.89	71.70	84.45	82.60	83.52	6719
36	AgeLess16	92.28	78.95	92.18	84.62	88.24	195
37	Age17-30	85.96	72.79	83.46	85.06	84.25	9507
38	Age31-45	86.26	77.91	88.10	87.08	87.59	12008
39	Female	98.85	97.05	98.69	98.31	98.50	6993
40	BodyFat	80.11	50.01	67.26	66.10	66.68	3352
41	BodyNormal	73.15	78.36	84.82	91.14	87.87	15919
42	BodyThin	72.97	37.04	59.44	49.57	54.06	2109
43	Customer	95.17	98.92	99.33	99.58	99.46	20250
44	Employee	98.00	90.88	94.06	96.41	95.22	1364
45	action-Calling	95.64	85.77	93.18	91.52	92.34	731
46	action-Talking	59.46	16.03	46.13	19.72	27.63	725
47	action-Gathering	68.52	31.02	58.40	39.83	47.36	1946
48	action-Holding	79.66	49.00	72.94	59.89	65.77	531
49	action-Pushing	90.66	67.48	79.54	81.66	80.58	338
50	action-Pulling	89.11	66.32	80.96	78.57	79.75	407
51	action-CarryingByArm	84.18	59.18	80.98	68.74	74.36	483
52	action-CarryingByHand	93.65	77.79	85.81	89.28	87.51	2568
53	action-Other	52.54	5.04	85.71	5.08	9.60	118
Avg		86.59	80.74	88.40	89.22	88.81	

Table 19: RAPv2 test results per attribute

Attribute Number	Attribute Name	ma	Acc	Prec	Rec	F1	Num images
1	hs-BaldHead	89.21	67.77	83.20	78.52	80.79	391
2	hs-LongHair	96.08	85.15	89.23	94.90	91.98	13129
3	hs-BlackHair	87.94	96.49	98.37	98.06	98.22	63314
4	hs-Hat	94.47	82.71	92.06	89.06	90.54	1042
5	hs-Glasses	93.02	71.70	79.79	87.61	83.52	4506
6	ub-Shirt	93.15	79.63	87.50	89.85	88.66	14701
7	ub-Sweater	79.83	45.25	61.66	62.96	62.30	5276
8	ub-Vest	96.75	88.26	93.70	93.82	93.76	3220
9	ub-TShirt	86.97	63.85	73.50	82.94	77.93	15726
10	ub-Cotton	90.28	68.09	78.64	83.54	81.01	7881
11	ub-Jacket	90.77	74.37	81.24	89.78	85.30	19346
12	ub-SuitUp	90.11	68.60	81.97	80.78	81.37	2067
13	ub-Tight	85.86	58.84	75.48	72.74	74.09	2837
14	ub-ShortSleeve	96.36	85.19	90.27	93.80	92.00	6561
15	ub-Others	58.28	14.12	44.29	17.17	24.75	1852
16	lb-LongTrousers	92.85	88.02	94.98	92.31	93.63	39118
17	lb-Skirt	88.53	62.11	75.47	77.83	76.63	2018
18	lb-ShortSkirt	92.76	71.48	80.94	85.95	83.37	1390
19	lb-Dress	90.72	61.58	70.89	82.42	76.22	1900
20	lb-Jeans	94.77	83.67	88.35	94.04	91.11	18081
21	lb-TightTrousers	94.79	77.54	83.09	92.07	87.35	8001
22	shoes-Leather	87.67	67.42	77.14	84.25	80.54	17877
23	shoes-Sports	80.82	50.50	62.18	72.90	67.11	13754
24	shoes-Boots	96.57	85.08	89.87	94.11	91.94	5741
25	shoes-Cloth	74.44	35.74	56.32	49.43	52.65	973
26	shoes-Casual	73.37	40.77	54.36	61.99	57.92	15393
27	shoes-Other	70.70	30.83	48.43	45.91	47.13	5740
28	attachment-Backpack	94.34	78.93	87.51	88.96	88.23	1449
29	attachment-ShoulderBag	94.15	79.43	87.87	89.22	88.54	4693
30	attachment-HandBag	89.59	66.36	79.82	79.73	79.78	1791
31	attachment-Box	89.82	67.26	80.42	80.42	80.42	2591
32	attachment-PlasticBag	89.39	66.82	80.92	79.31	80.11	1866
33	attachment-PaperBag	76.54	40.43	62.46	53.41	57.58	704
34	attachment-HandTrunk	96.17	82.26	87.99	92.66	90.26	1661
35	attachment-Other	87.38	69.80	82.09	82.34	82.21	20154
36	AgeLess16	90.34	73.45	89.03	80.76	84.70	603
37	Age17-30	80.86	62.84	76.58	77.79	77.18	27388
38	Age31-45	77.83	67.33	79.02	81.99	80.48	37188
39	Age46-60	68.71	27.80	49.42	38.87	43.51	2398
40	Female	98.65	96.31	98.06	98.18	98.12	21251
41	BodyFat	78.91	47.08	64.80	63.25	64.02	9271
42	BodyNormal	71.65	81.15	86.81	92.57	89.60	52852
43	BodyThin	69.09	30.15	53.12	41.09	46.34	5041
44	Customer	88.83	97.77	98.61	99.15	98.87	63782
45	Employee	93.74	77.75	86.73	88.25	87.48	3635
46	action-Calling	96.22	84.06	89.92	92.81	91.34	2296
47	action-Talking	58.95	15.04	44.33	18.54	26.15	1812
48	action-Gathering	65.94	25.54	51.94	33.44	40.69	3289
49	action-Holding	82.53	53.20	73.77	65.61	69.45	1582
50	action-Pushing	85.86	57.75	74.49	71.99	73.22	714
51	action-Pulling	90.67	69.34	82.13	81.66	81.90	1216
52	action-CarryingByArm	85.62	58.61	76.10	71.83	73.91	1729
53	action-CarryingByHand	92.02	73.66	82.99	86.76	84.83	9028
54	action-Other	61.71	20.12	57.75	23.60	33.50	695
Avg		85.60	76.27	84.98	86.80	85.88	

Table 20: RAPzs training results per attribute

Attribute Number	Attribute Name	ma	Acc	Prec	Rec	F1	Num images
1	hs-BaldHead	81.99	50.00	69.41	64.13	66.67	92
2	hs-LongHair	93.71	80.18	87.54	90.51	89.00	3276
3	hs-BlackHair	81.91	95.48	97.60	97.78	97.69	15860
4	hs-Hat	88.85	66.07	81.18	78.01	79.57	282
5	hs-Glasses	90.88	64.35	73.41	83.91	78.31	1125
6	ub-Shirt	88.98	68.74	79.07	84.03	81.47	3645
7	ub-Sweater	71.82	28.16	39.13	50.12	43.94	1303
8	ub-Vest	92.75	72.76	82.17	86.39	84.23	779
9	ub-TShirt	80.42	51.59	62.96	74.07	68.07	3957
10	ub-Cotton	83.23	49.69	61.60	71.98	66.39	1863
11	ub-Jacket	82.99	59.85	71.38	78.75	74.88	4889
12	ub-SuitUp	81.78	49.06	67.13	64.57	65.83	525
13	ub-Tight	74.83	36.29	55.00	51.61	53.25	746
14	ub-ShortSleeve	91.03	72.74	84.79	83.65	84.22	1633
15	ub-Others	53.19	5.68	23.44	6.98	10.75	430
16	lb-LongTrousers	88.30	81.32	91.31	88.14	89.70	9840
17	lb-Skirt	78.15	40.20	57.11	57.58	57.35	488
18	lb-ShortSkirt	80.95	45.49	62.36	62.71	62.54	354
19	lb-Dress	79.31	40.70	55.78	60.08	57.85	506
20	lb-Jeans	91.31	74.83	81.93	89.62	85.60	4442
21	lb-TightTrousers	90.89	68.04	77.26	85.08	80.98	1977
22	shoes-Leather	84.44	60.13	69.64	81.48	75.10	4449
23	shoes-Sports	78.90	45.38	54.50	73.07	62.43	3401
24	shoes-Boots	93.93	74.28	81.21	89.70	85.24	1378
25	shoes-Cloth	74.82	34.11	51.36	50.38	50.87	262
26	shoes-Casual	68.85	34.95	50.31	53.38	51.80	3895
27	shoes-Other	58.65	15.78	45.66	19.43	27.26	1436
28	attachment-Backpack	87.17	59.01	73.53	74.93	74.22	367
29	attachment-ShoulderBag	87.13	60.20	74.08	76.26	75.16	1188
30	attachment-HandBag	81.68	47.19	63.90	64.33	64.12	443
31	attachment-Box	80.70	45.61	62.37	62.93	62.65	661
32	attachment-PlasticBag	78.61	39.94	55.80	58.41	57.08	428
33	attachment-PaperBag	70.97	27.30	43.26	42.54	42.90	181
34	attachment-HandTrunk	89.46	64.35	77.14	79.52	78.31	420
35	attachment-Other	80.62	56.76	71.02	73.87	72.42	5013
36	AgeLess16	83.56	54.01	73.19	67.33	70.14	150
37	Age17-30	72.95	51.48	65.61	70.50	67.97	6790
38	Age31-45	70.04	57.99	73.09	73.73	73.41	9402
39	Age46-60	59.26	14.85	37.84	19.65	25.87	570
40	Female	97.13	92.17	95.58	96.27	95.93	5284
41	BodyFat	68.70	29.67	45.46	46.07	45.77	2305
42	BodyNormal	62.18	72.71	82.79	85.66	84.20	13161
43	BodyThin	62.75	19.09	33.75	30.52	32.05	1314
44	Customer	84.08	96.82	98.05	98.72	98.39	15961
45	Employee	87.95	63.74	78.64	77.08	77.85	903
46	action-Calling	89.76	65.41	77.96	80.26	79.09	542
47	action-Talking	55.52	9.00	26.70	11.96	16.52	460
48	action-Gathering	61.28	16.43	31.87	25.33	28.23	829
49	action-Holding	72.08	31.05	49.62	45.35	47.39	430
50	action-Pushing	85.92	49.59	61.22	72.29	66.30	166
51	action-Pulling	80.89	48.90	69.44	62.31	65.68	321
52	action-CarryingByArm	75.86	34.84	50.33	53.10	51.68	435
53	action-CarryingByHand	86.86	60.87	73.59	77.88	75.67	2197
54	action-Other	58.48	13.30	36.71	17.26	23.48	168
Avg		79.23	67.31	78.39	80.64	79.50	

Table 21: RAPzs test results per attribute

Attribute Number	Attribute Name	ma	Acc	Prec	Rec	F1	Num images
1	hs-BaldHead	74.93	23.08	30.00	50.00	37.50	6
2	hs-LongHair	92.54	79.93	89.03	88.66	88.84	1217
3	hs-BlackHair	79.19	96.75	98.14	98.56	98.35	4709
4	hs-Hat	86.19	63.10	82.81	72.60	77.37	73
5	hs-Glasses	86.63	62.43	78.47	75.33	76.87	450
6	ub-Shirt	86.70	67.83	83.19	78.60	80.83	1215
7	ub-Sweater	66.88	26.30	38.75	45.02	41.65	673
8	ub-Vest	86.02	66.46	87.50	73.43	79.85	572
9	ub-TShirt	74.77	44.36	58.15	65.18	61.46	1232
10	ub-Cotton	82.28	52.86	67.98	70.38	69.16	736
11	ub-Jacket	79.06	51.44	63.37	73.20	67.93	1295
12	ub-SuitUp	81.38	50.00	70.30	63.39	66.67	112
13	ub-Tight	64.14	20.44	38.24	30.52	33.94	213
14	ub-ShortSleeve	68.23	24.39	41.67	37.04	39.22	54
15	ub-Others	50.00	0.00	0.00	0.00	0.00	6
16	lb-LongTrousers	86.68	77.63	87.17	87.64	87.41	2590
17	lb-Skirt	72.90	34.15	55.56	46.98	50.91	149
18	lb-ShortSkirt	73.37	34.50	55.20	47.92	51.30	144
19	lb-Dress	76.91	41.40	62.68	54.94	58.55	162
20	lb-Jeans	90.56	76.44	85.72	87.59	86.65	1515
21	lb-TightTrousers	87.15	66.27	82.46	77.15	79.72	731
22	shoes-Leather	85.49	65.90	78.30	80.62	79.44	1486
23	shoes-Sports	75.47	47.20	64.06	64.20	64.13	1327
24	shoes-Boots	92.58	78.44	88.78	87.07	87.92	727
25	shoes-Cloth	51.89	2.78	8.33	4.00	5.41	25
26	shoes-Casual	68.65	30.71	43.49	51.12	47.00	849
27	shoes-Other	50.00	0.00	0.00	0.00	0.00	2
28	attachment-Backpack	73.47	38.79	68.18	47.37	55.90	95
29	attachment-ShoulderBag	79.38	46.49	66.81	60.46	63.47	263
30	attachment-HandBag	79.58	43.59	61.15	60.28	60.71	141
31	attachment-Box	78.57	43.73	63.21	58.65	60.85	208
32	attachment-PlasticBag	70.37	30.51	53.73	41.38	46.75	87
33	attachment-PaperBag	53.42	4.88	12.50	7.41	9.30	54
34	attachment-HandTrunk	84.41	51.97	67.35	69.47	68.39	95
35	attachment-Other	76.40	50.45	69.56	64.75	67.07	1461
36	AgeLess16	76.29	41.86	66.67	52.94	59.02	68
37	Age17-30	69.46	49.02	67.93	63.78	65.79	2228
38	Age31-45	70.43	57.55	71.77	74.39	73.06	2632
39	Female	95.43	88.89	94.20	94.04	94.12	1745
40	BodyFat	59.85	19.31	38.73	27.81	32.37	766
41	BodyNormal	57.24	67.96	76.57	85.81	80.93	3602
42	BodyThin	61.66	18.87	34.37	29.51	31.75	488
43	Customer	86.68	97.79	98.68	99.08	98.88	4687
44	Employee	89.27	67.56	81.94	79.37	80.64	223
45	action-Calling	87.72	61.74	76.17	76.53	76.35	213
46	action-Talking	57.93	11.79	26.73	17.42	21.09	155
47	action-Gathering	63.43	20.75	37.50	31.73	34.38	416
48	action-Holding	66.70	21.32	35.29	35.00	35.15	120
49	action-Pushing	63.64	11.90	17.24	27.78	21.28	18
50	action-Pulling	81.42	46.92	64.21	63.54	63.87	96
51	action-CarryingByArm	61.77	15.07	27.85	24.72	26.19	89
52	action-CarryingByHand	81.04	53.12	74.22	65.14	69.38	588
53	action-Other	49.98	0.00	0.00	0.00	0.00	16
Avg		74.46	65.62	78.22	78.26	78.24	

C.2. Attribute scores per dataset

Table 22: Attribute Scores for RAPv1

Attribute Number	Attribute Name	Low Training Images	Test performance	Drop in Performance	Score
1	hs-BaldHead	True	Low	Big	0
2	hs-LongHair	False	High	Small	6
3	hs-BlackHair	False	High	Small	6
4	hs-Hat	True	Medium	Medium	2
5	hs-Glasses	False	Medium	Small	5
6	hs-Muffler	True	Low	Big	0
7	ub-Shirt	False	High	Small	6
8	ub-Sweater	False	Low	Medium	3
9	ub-Vest	False	High	Small	6
10	ub-TShirt	False	Medium	Medium	4
11	ub-Cotton	False	Medium	Medium	4
12	ub-Jacket	False	Medium	Medium	4
13	ub-SuitUp	True	Medium	Medium	2
14	ub-Tight	True	Medium	Big	1
15	ub-ShortSleeve	True	Medium	Medium	2
16	lb-LongTrousers	False	High	Small	6
17	lb-Skirt	False	High	Small	6
18	lb-ShortSkirt	True	Medium	Medium	2
19	lb-Dress	False	Medium	Medium	4
20	lb-Jeans	False	High	Small	6
21	lb-TightTrousers	False	High	Small	6
22	shoes-Leather	False	Medium	Small	5
23	shoes-Sport	False	Medium	Small	5
24	shoes-Boots	False	High	Small	6
25	shoes-Cloth	True	Medium	Small	3
26	shoes-Casual	False	Low	Medium	3
27	attach-Backpack	True	Medium	Medium	2
28	attach-SingleShoulderBag	False	Medium	Medium	4
29	attach-HandBag	True	Medium	Medium	2
30	attach-Box	False	Medium	Medium	4
31	attach-PlasticBag	True	Medium	Medium	2
32	attach-PaperBag	True	Low	Medium	1
33	attach-HandTrunk	True	Medium	Medium	2
34	attach-Other	False	Medium	Medium	4
35	AgeLess16	True	Medium	Medium	2
36	Age17-30	False	Medium	Medium	4
37	Age31-45	False	Medium	Small	5
38	Female	False	High	Small	6
39	BodyFat	False	Low	Big	2
40	BodyNormal	False	High	Small	6
41	BodyThin	False	Low	Big	2
42	Customer	False	High	Small	6
43	Clerk	False	High	Small	6
44	action-Calling	False	Medium	Medium	4
45	action-Talking	False	Low	Medium	3
46	action-Gathering	False	Low	Medium	3
47	action-Holding	True	Low	Big	0
48	action-Pushing	True	Medium	Small	3
49	action-Pulling	True	Medium	Medium	2
50	action-CarrybyArm	True	Low	Big	0
51	action-CarrybyHand	False	Medium	Small	5

Table 23: Attribute Scores for RAPv2

Attribute Number	Attribute Name	Low Training Images	Test performance	Drop in Performance	Score
1	hs-BaldHead	True	Medium	Small	3
2	hs-LongHair	False	High	Small	6
3	hs-BlackHair	False	High	Small	6
4	hs-Hat	True	Medium	Small	3
5	hs-Glasses	False	Medium	Small	5
6	ub-Shirt	False	High	Small	6
7	ub-Sweater	False	Low	Medium	3
8	ub-Vest	False	High	Small	6
9	ub-TShirt	False	Medium	Small	5
10	ub-Cotton	False	Medium	Small	5
11	ub-Jacket	False	Medium	Small	5
12	ub-SuitUp	False	Medium	Medium	4
13	ub-Tight	False	Medium	Medium	4
14	ub-ShortSleeve	False	High	Small	6
15	ub-Others	True	Low	Small	2
16	lb-LongTrousers	False	High	Small	6
17	lb-Skirt	True	Medium	Medium	2
18	lb-ShortSkirt	True	Medium	Medium	2
19	lb-Dress	True	Medium	Medium	2
20	lb-Jeans	False	High	Small	6
21	lb-TightTrousers	False	High	Small	6
22	shoes-Leather	False	Medium	Small	5
23	shoes-Sports	False	Medium	Small	5
24	shoes-Boots	False	High	Small	6
25	shoes-Cloth	True	Medium	Small	3
26	shoes-Casual	False	Medium	Small	5
27	shoes-Other	False	Low	Medium	3
28	attachment-Backpack	True	Medium	Small	3
29	attachment-ShoulderBag	False	Medium	Small	5
30	attachment-HandBag	True	Medium	Medium	2
31	attachment-Box	False	Medium	Medium	4
32	attachment-PlasticBag	True	Medium	Medium	2
33	attachment-PaperBag	True	Low	Small	2
34	attachment-HandTrunk	True	Medium	Small	3
35	attachment-Other	False	Medium	Small	5
36	AgeLess16	True	Medium	Small	3
37	Age17-30	False	Medium	Small	5
38	Age31-45	False	Medium	Small	5
39	Age46-60	False	Low	Medium	3
40	Female	False	High	Small	6
41	BodyFat	False	Low	Medium	3
42	BodyNormal	False	High	Small	6
43	BodyThin	False	Low	Small	4
44	Customer	False	High	Small	6
45	Employee	False	Medium	Small	5
46	action-Calling	False	Medium	Small	5
47	action-Talking	True	Low	Small	2
48	action-Gathering	False	Low	Small	4
49	action-Holding	True	Low	Medium	1
50	action-Pushing	True	Medium	Small	3
51	action-Pulling	True	Medium	Medium	2
52	action-CarryingByArm	True	Medium	Medium	2
53	action-CarryingByHand	False	Medium	Small	5
54	action-Other	True	Low	Small	2

Table 24: Attribute Scores for RAPzs

Attribute Number	Attribute Name	Low Training Images	Test performance	Drop in Performance	Score
1	hs-BaldHead	True	Low	Big	0
2	hs-LongHair	False	High	Small	6
3	hs-BlackHair	False	High	Small	6
4	hs-Hat	True	Medium	Small	3
5	hs-Glasses	False	Medium	Small	5
6	ub-Shirt	False	High	Small	6
7	ub-Sweater	False	Low	Medium	3
8	ub-Vest	False	Medium	Medium	4
9	ub-TShirt	False	Medium	Medium	4
10	ub-Cotton	False	Medium	Medium	4
11	ub-Jacket	False	Medium	Medium	4
12	ub-SuitUp	True	Medium	Medium	2
13	ub-Tight	False	Low	Big	2
14	ub-ShortSleeve	True	Low	Big	0
15	ub-Others	True	Low	Small	2
16	lb-LongTrousers	False	High	Small	6
17	lb-Skirt	False	Medium	Big	3
18	lb-ShortSkirt	True	Medium	Big	1
19	lb-Dress	False	Medium	Medium	4
20	lb-Jeans	False	High	Small	6
21	lb-TightTrousers	False	Medium	Small	5
22	shoes-Leather	False	Medium	Small	5
23	shoes-Sports	False	Medium	Small	5
24	shoes-Boots	False	High	Small	6
25	shoes-Cloth	True	Low	Big	0
26	shoes-Casual	False	Low	Small	4
27	shoes-Other	True	Low	Small	2
28	attachment-Backpack	True	Medium	Medium	2
29	attachment-ShoulderBag	False	Medium	Medium	4
30	attachment-HandBag	True	Medium	Medium	2
31	attachment-Box	False	Medium	Medium	4
32	attachment-PlasticBag	True	Low	Medium	1
33	attachment-PaperBag	True	Low	Medium	1
34	attachment-HandTrunk	False	Medium	Medium	4
35	attachment-Other	False	Medium	Medium	4
36	AgeLess16	True	Medium	Medium	2
37	Age17-30	False	Medium	Medium	4
38	Age31-45	False	Medium	Small	5
39	Age46-60	False	High	Small	6
40	Female	False	Low	Big	2
41	BodyFat	False	High	Small	6
42	BodyNormal	False	Low	Medium	3
43	BodyThin	False	High	Small	6
44	Customer	False	High	Small	6
45	Employee	False	Medium	Medium	4
46	action-Calling	False	Low	Small	4
47	action-Talking	False	Low	Small	4
48	action-Gathering	True	Low	Big	0
49	action-Holding	True	Low	Big	0
50	action-Pushing	True	Medium	Medium	2
51	action-Pulling	True	Low	Big	0
52	action-CarryingByArm	False	Medium	Medium	4
53	action-CarryingByHand	True	Low	Small	2
54	action-Other	False	Low	Small	4

C.3. Critical attributes per dataset

Table 25: Score per attribute RAPv1

Score	Attribute Number	Attribute Name
0	1	hs-BaldHead
	6	hs-Muffler
	47	action-Holding
	50	action-CarrybyArm
1	14	ub-Tight
	32	attach-PaperBag
2	4	hs-Hat
	13	ub-SuitUp
	15	ub-ShortSleeve
	18	lb-ShortSkirt
	27	attach-Backpack
	29	attach-HandBag
	31	attach-PlasticBag
	33	attach-HandTrunk
	35	AgeLess16
	39	BodyFat
	41	BodyThin
	49	action-Pulling
3	8	ub-Sweater
	25	shoes-Cloth
	26	shoes-Casual
	45	action-Talking
	46	action-Gathering
	48	action-Pusing
	10	ub-TShirt
4	11	ub-Cotton
	12	ub-Jacket
	19	lb-Dress
	28	attach-SingleShoulderBag
	30	attach-Box
	34	attach-Other
	36	Age17-30
	44	action-Calling
	5	hs-Glasses
	22	shoes-Leather
5	23	shoes-Sport
	37	Age31-45
	51	action-CarrybyHand
	2	hs-LongHair
	3	hs-BlackHair
6	7	ub-Shirt
	9	ub-Vest
	16	lb-LongTrousers
	17	lb-Skirt
	20	lb-Jeans
	21	lb-TightTrousers
	24	shoes-Boots
	38	Female
	40	BodyNormal
	42	Customer
	43	Clerk

Table 26: Score per attribute RAPv2

Score	Attribute Number	Attribute Name
1	49	action-Holding
	15	ub-Others
	17	lb-Skirt
	18	lb-ShortSkirt
	19	lb-Dress
	30	attachment-HandBag
	32	attachment-PlasticBag
	33	attachment-PaperBag
	47	action-Talking
	51	action-Pulling
	52	action-CarryingByArm
	54	action-Other
3	1	hs-BaldHead
	4	hs-Hat
	7	ub-Sweater
	25	shoes-Cloth
	27	shoes-Other
	28	attachment-Backpack
	34	attachment-HandTrunk
	36	AgeLess16
	39	Age46-60
	41	BodyFat
	50	action-Pushing
	12	ub-SuitUp
4	13	ub-Tight
	31	attachment-Box
	43	BodyThin
	48	action-Gathering
	5	hs-Glasses
	9	ub-TShirt
	10	ub-Cotton
	11	ub-Jacket
	22	shoes-Leather
	23	shoes-Sports
	26	shoes-Casual
	29	attachment-ShoulderBag
5	35	attachment-Other
	37	Age17-30
	38	Age31-45
	45	Employee
	46	action-Calling
	53	action-CarryingByHand
	2	hs-LongHair
	3	hs-BlackHair
	6	ub-Shirt
	8	ub-Vest
	14	ub-ShortSleeve
	16	lb-LongTrousers
6	20	lb-Jeans
	21	lb-TightTrousers
	24	shoes-Boots
	40	Female
	42	BodyNormal
	44	Customer

Table 27: Score per attribute RAPzs

Score	Attribute Number	Attribute Name
0	1	hs-BaldHead
	14	ub-ShortSleeve
	25	shoes-Cloth
	48	action-Gathering
	49	action-Holding
	51	action-Pulling
1	18	lb-ShortSkirt
	32	attachment-PlasticBag
	33	attachment-PaperBag
2	12	ub-SuitUp
	13	ub-Tight
	15	ub-Others
	27	shoes-Other
	28	attachment-Backpack
	30	attachment-HandBag
	36	AgeLess16
	40	Female
	50	action-Pushing
	53	action-CarryingByHand
3	4	hs-Hat
	7	ub-Sweater
	17	lb-Skirt
	42	BodyNormal
4	8	ub-Vest
	9	ub-TShirt
	10	ub-Cotton
	11	ub-Jacket
	19	lb-Dress
	26	shoes-Casual
	29	attachment-ShoulderBag
	31	attachment-Box
	34	attachment-HandTrunk
	35	attachment-Other
	37	Age17-30
	45	Employee
	46	action-Calling
	47	action-Talking
	52	action-CarryingByArm
	54	action-Other
5	5	hs-Glasses
	21	lb-TightTrousers
	22	shoes-Leather
	23	shoes-Sports
	38	Age31-45
6	2	hs-LongHair
	3	hs-BlackHair
	6	ub-Shirt
	16	lb-LongTrousers
	20	lb-Jeans
	24	shoes-Boots
	39	Age46-60
	41	BodyFat
	43	BodyThin
	44	Customer

C.4. Critical attributes final results

Table 28: Top 20 Worse Attributes per Dataset

Lower	R _{API} Attribute Number	R _{API} Attribute Name	R _{AP2} Attribute Number	R _{AP2} Attribute Name	R _{APZS} Attribute Number	R _{APZS} Attribute Name
1	1	hs-BaldHead	49	action-Holding	1	hs-BaldHead
2	6	hs-Muffler	15	ub-Others	14	ub-ShortSleeve
3	47	action-Holding	17	lb-Skirt	25	shoes-Cloth
4	50	action-CarrybyArm	18	lb-ShortSkirt	48	action-Gathering
5	14	ub-Tight	19	lb-Dress	49	action-Holding
6	32	attach-PaperBag	30	attachment-HandBag	51	action-Pulling
7	4	hs-Hat	32	attachment-PlasticBag	18	lb-ShortSkirt
8	13	ub-SuitUp	33	attachment-PaperBag	32	attachment-PlasticBag
9	15	ub-ShortSleeve	47	action-Talking	33	attachment-PaperBag
10	18	lb-ShortSkirt	51	action-Pulling	12	ub-SuitUp
11	27	attach-Backpack	52	action-CarryingByArm	13	ub-Tight
12	29	attach-HandBag	54	action-Other	15	ub-Others
13	31	attach-PlasticBag	1	hs-BaldHead	27	shoes-Other
14	33	attach-HandTrunk	4	hs-Hat	28	attachment-Backpack
15	35	AgeLess16	7	ub-Sweater	30	attachment-HandBag
16	39	BodyFat	25	shoes-Cloth	36	AgeLess16
17	41	BodyThin	27	shoes-Other	40	Female
18	49	action-Pulling	28	attachment-Backpack	50	action-Pushing
19	8	ub-Sweater	34	attachment-HandTrunk	53	action-CarryingByHand
20	25	shoes-Cloth	36	AgeLess16	4	hs-Hat

Table 29: Number of datasets where each attribute is on the top-worse attributes

Attribute Number	Attribute Name	Times as Top-Worse Attribute
49	action-Holding	3
51	action-Pulling	3
1	hs-BaldHead	3
18	lb-ShortSkirt	3
36	AgeLess16	3
4	hs-Hat	3
25	shoes-Cloth	3
7	ub-Sweater	2
12	ub-SuitUp	2
13	ub-Tight	2
28	attachment-Backpack	2
30	attachment-HandBag	2
33	attachment-PlasticBag	2
32	attachment-PaperBag	2
27	shoes-Other	2
15	ub-Others	2
14	ub-ShortSleeve	2
41	BodyFat	1
48	action-Gathering	1
19	lb-Dress	1
50	action-Pushing	1
47	action-Talking	1
43	BodyThin	1
17	lb-Skirt	1
52	action-CarryingByArm	1
53	action-CarryingByHand	1
54	action-Other	1
40	attachment-HandTrunk	1
34	shoes-Casual	0
36	Age46-60	0
9	ub-TShirt	0
10	ub-Cotton	0
11	attachment-Box	0
23	attachment-ShoulderBag	0
42	BodyNormal	0
5	hs-Glasses	0
8	ub-Vest	0
4	action-Calling	0
37	Age17-30	0
38	Age35-45	0
35	attachment-Other	0
44	Employee	0
45	Customer	0
3	hs-BlackHair	0
2	hs-LongHair	0
16	lb-Jeans	0
21	lb-LongTrousers	0
22	lb-TightTrousers	0
24	shoes-Boots	0
23	shoes-Leather	0
6	shoes-Sports	0

D. Extended experimental results for Synthetic Data Augmentation

D.1. Parameter Selection for Generation

To optimize augmentation, we selected the weakest attribute *hs-BaldHead* identified by our approach, and we evaluated three key parameters: image noise level, augmented weight, and the number of images added to the dataset, represented as the percentage of number of images added relative to the number of images the attribute has in the training set. For example, *hs-BaldHead* in RAPv1 has 122 images in training; an augmentation percentage of 50% represents adding 66 synthetic images to the training set with this attribute.

The augmented weight is designed to influence the dataset's overall results, as its value is only parameterizable for attributes labeled as 3 (the indirectly augmented ones). For this reason, finding an optimal value for it has been reserved for later.

With this in mind, the first step was to analyze the relationship between the level of noise in the image and the percentage of augmentation applied to the attribute, keeping the augmented weight fixed at 0.5. Based on the results yielding the best performance, further experiments were proposed to observe the effect of varying the augmented weight. For this purpose, three levels of noise were configured, modifying how much blending of the generated noise occurs in the image (at 25%, 50%, or 75%). Initially, augmentation levels of 50%, 100%, 200%, and 300% were configured. However, after observing the initial results, additional values between 400% and 700% were tested.

The training processes were conducted to ensure that the only differences between the various parameter configurations were those directly influencing the parameters themselves. Specifically, noise levels were added to the same base image, meaning that image 1 of *small_noise* and image 1 of *big_noise* are identical except for the noise level. Similarly, augmentation was applied using overlapping sets, such that 100% augmentation includes as first half the 50% set, 200% includes the 100% set, and so forth. All results computed are available in Tables 30, 31 and 32.

Table 30: Performance results for data augmentation of *hs-BaldHead* in RAPv1

% Augmentation	Noise	Aug. Weight	BaldHead					All Attributes				
			ma	Acc	Prec	Rec	F1	ma	Acc	Prec	Rec	F1
50	Big	0.5	73.56	37.78	65.38	47.22	54.84	80.50	68.43	80.03	80.54	80.28
100	Big	0.5	81.87	46.94	63.89	63.89	63.89	81.15	68.39	79.76	80.75	80.25
200	Big	0.5	77.71	42.55	64.52	55.56	59.70	80.51	68.74	80.05	80.88	80.46
300	Big	0.5	77.71	41.67	62.50	55.56	58.82	80.48	68.27	79.68	80.69	80.18
400	Big	0.5	77.70	40.82	60.61	55.56	57.97	80.91	68.47	79.64	81.02	80.33
500	Big	0.5	73.54	36.17	60.71	47.22	53.12	80.41	68.27	79.40	80.91	80.14
600	Big	0.5	77.72	43.48	66.67	55.56	60.61	80.95	68.65	79.86	81.07	80.46
700	Big	0.5	76.31	38.78	59.38	52.78	55.88	80.94	68.54	79.54	81.25	80.39
50	Medium	0.5	76.31	38.78	59.38	52.78	55.88	80.56	68.48	79.92	80.75	80.34
100	Medium	0.5	77.72	43.48	66.67	55.56	60.61	80.62	68.60	80.03	80.72	80.37
200	Medium	0.5	77.72	44.44	68.97	55.56	61.54	80.24	68.54	79.98	80.72	80.35
300	Medium	0.5	77.71	42.55	64.52	55.56	59.70	80.84	68.88	79.96	81.29	80.62
400	Medium	0.5	77.72	44.44	68.97	55.56	61.54	80.83	68.34	79.78	80.65	80.21
500	Medium	0.5	77.74	46.51	74.07	55.56	63.49	80.97	68.65	79.56	81.38	80.46
600	Medium	0.5	74.93	38.30	62.07	50.00	55.38	81.09	68.92	79.97	81.32	80.64
700	Medium	0.5	74.91	35.29	54.55	50.00	52.17	80.77	68.71	79.62	81.37	80.49
50	Small	0.5	74.94	39.13	64.29	50.00	56.25	80.84	68.68	79.99	80.95	80.47
100	Small	0.5	80.49	46.81	66.67	61.11	63.77	80.87	68.46	79.94	80.67	80.30
200	Small	0.5	77.71	41.67	62.50	55.56	58.82	80.38	68.60	79.86	80.90	80.37
300	Small	0.5	79.11	46.67	70.00	58.33	63.64	80.41	68.44	79.85	80.70	80.27
400	Small	0.5	74.92	36.00	56.25	50.00	52.94	80.81	68.44	79.68	80.89	80.28
500	Small	0.5	73.58	41.46	77.27	47.22	58.62	80.32	68.26	79.31	80.97	80.13
600	Small	0.5	73.56	37.78	65.38	47.22	54.84	80.77	68.74	79.91	81.11	80.51
700	Small	0.5	74.95	40.91	69.23	50.00	58.06	80.61	68.48	79.56	81.11	80.32

The first parameter to set was the augmentation percentage. Figure 11 shows the results obtained on *hs-BaldHead* on RAPv1 for all different levels of noise on the previously mentioned percentages. Based on these observations, even if improvements are achieved in all cases, with some being almost 20 points better in the selected metric, it was decided to

Table 31: Performance results for data augmentation of *hs-BaldHead* in RAPv2

% Augmentation	Noise	Aug. Weight	BaldHead					All Attributes				
			ma	Acc	Prec	Rec	F1	ma	Acc	Prec	Rec	F1
50	Medium	0.5	80.62	46.905	66.68	61.41	63.86	78.88	67.265	78.59	80.33	79.45
100	Medium	0.5	81.46	51.79	74.36	63.04	68.24	78.96	67.16	78.16	80.64	79.38
200	Medium	0.5	83.33	49.395	65.425	66.845	66.13	79.195	67.375	78.48	80.65	79.55
300	Medium	0.5	82.53	50.42	68.97	65.22	67.04	79.18	67.30	78.06	80.98	79.49
400	Medium	0.5	79.55	47.215	69.935	59.24	64.135	79.135	67.67	78.21	81.42	79.78
500	Medium	0.5	83.08	51.69	70.11	66.30	68.16	79.50	67.58	78.02	81.49	79.72

Table 32: Performance results for data augmentation of *hs-BaldHead* in RAPzs

% Augmentation	Noise	Aug. Weight	BaldHead					All Attributes				
			ma	Acc	Prec	Rec	F1	ma	Acc	Prec	Rec	F1
50	Medium	0.5	66.61	16.67	25.00	33.33	28.57	73.42	65.82	78.58	78.09	78.34
100	Medium	0.5	74.93	23.08	30.00	50.00	37.50	74.16	65.37	77.92	78.20	78.06
200	Medium	0.5	66.60	15.38	22.22	33.33	26.67	73.67	65.06	77.68	77.91	77.79
300	Medium	0.5	66.64	22.22	40.00	33.33	36.36	73.53	65.45	77.78	78.41	78.09
400	Medium	0.5	66.64	22.22	40.00	33.33	36.36	73.56	65.72	78.22	78.32	78.27
500	Medium	0.5	66.65	25.00	50.00	33.33	40.00	73.49	65.39	77.84	78.28	78.06

restrict the augmentation percentage to 500%, since higher values do not yield improvements and significantly reduce the number of images to generate and the generation time required.

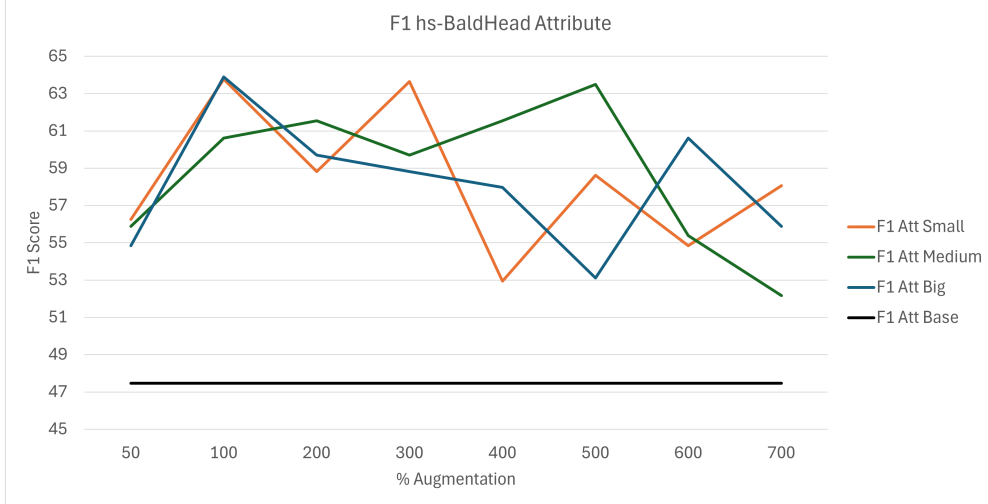


Figure 11: Results for hs-BaldHead depending on the noise level for each augmentation percentage on the attribute

Regarding each noise levels, small and big noise exhibit less stable behavior, with their minimum and maximum values falling within similar ranges to the other augmentations but without displaying clear trends. On the other hand, medium noise appears to show a trend of improvement as more images are added, which is expected, until reaching 500% augmentation, at which point a decline begins.

As shown in Table 33, for the specific attribute evaluated, the medium noise level yields the highest average performance. This finding demonstrates that the introduction of noise is beneficial, indicating that a minimal amount of noise is insufficient, while simultaneously confirming that an excessive noise level degrades performance.

For these reasons, it was decided to fix the maximum augmentation percentage in 500%, and the level of noise in the medium one, and with these configurations, the next step was to search for an optimal augmented weight. Various augmented weights between 0 and 1 were tested, resulting in the outcomes shown in Table 34.

Table 33: Attribute-level F1-score comparison of noise levels for *hs-BaldHead* attribute on the RAP datasets. An augmentation weight of 0.5 was employed.

Noise level	RAPv1	RAPv2	RAPzs
Big noise (75%)	53.12	66.67	23.53
Medium noise (50%)	63.49	68.16	40.00
Small noise (25%)	58.62	66.29	40.00
Optimized baseline results	47.46	66.67	37.50

Table 34: Attribute-level F1-score comparison of augmentation weights for *hs-BaldHead* attribute on the RAP datasets. A medium noise level was employed.

Augmentation Weight	RAPv1	RAPv2	RAPzs
0.25	61.29	65.17	14.29
0.5	63.49	68.16	40.00
0.75	53.33	64.77	40.00
1	54.24	65.90	18.18
Optimized baseline results	47.46	66.67	37.50

Table 35: Comparison of F1 on the attribute and F1 on the Dataset for the hs-BaldHead attribute across RAPv1, RAPv2, and RAPzs datasets for different data augmentation (DA) percentages.

DA (%)	RAPv1		RAPv2		RAPzs	
	F1 Attribute	F1 Dataset	F1 Attribute	F1 Dataset	F1 Attribute	F1 Dataset
50	55.88	80.34	63.86	79.45	28.57	78.34
100	60.61	80.37	68.24	79.38	37.50	78.06
200	61.54	80.35	66.13	79.55	26.67	77.79
300	59.70	80.62	67.04	79.49	36.36	78.09
400	61.54	80.21	64.14	79.78	36.36	78.27
500	63.49	80.46	68.16	79.72	40.00	78.06
Optimized baseline results	47.46	80.30	66.67	79.38	37.50	78.20

Table 36: Number of hs-BaldHead train and test images for RAP datasets.

Dataset	# hs-BaldHead Train Images	# hs-BaldHead Test Images
RAPv1	122	36
RAPv2	391	92
RAPzs	116	6

As can be observed, the best result is obtained with the default value previously tested. This confirms that the decision to treat attributes labeled as 3 with different weights is well-founded, as scores degrade when these attributes are given either full or zero weight. Also, it can be noted how indeed the other attributes are somehow noisy or not fully representative, and therefore 1 is not the best value for this parameter.

In any case, these final results conclude the selection of general hyperparameters for obtaining results on the other datasets. The selected configuration includes medium noise, an augmented weight of 0.5, and augmentation percentages of 50%, 100%, 200%, 300%, 400% and 500%.

On hs-BaldHead results: Overall, Table 35 presents the final results on the attribute, revealing that incorporating augmentation consistently enhances performance across all datasets. For both RAPv1 and RAPv2, similar trends are observed, with notable performance gains achieved at 500% augmentation, although for RAPv2 a slight edge is seen at 100% augmentation.

In contrast, the zero-shot setting exhibits much less pronounced improvements. While the optimal augmentation percentage remains consistent with the previous cases, the overall performance boost relative to the baseline is minimal, particularly given the low starting performance.

A likely contributing factor is that, as shown in Table 36, the *hs-BaldHead* class comprises only 6 images in the testing set. To further investigate the model’s failure modes and assess their representativeness, we examined the ground truth annotations and analyzed the predicted probabilities, with the corresponding findings presented in Figure 12.

As observed, the model correctly predicts half of the ground truth images, which aligns with the reported metrics. However, a closer examination of the ground truth reveals that, despite the testing set comprising only 6 images, the dataset is noisy; notably, 3 of these images depict individuals with hair. For instance, image 1518 (bottom left) might be considered bald since, despite the presence of hair, the scalp is visible at the top of the head. In contrast, the two images in the rightmost column clearly show pedestrians with full heads of hair, one of which features untrimmed, short hair. Thus, the inability of the model to achieve better results on RAPzs is justified. The combination of a very small test set and significant noise in the annotations contributes to the observed discrepancies between the predictions and the expected ground truth.

Results on *lb-ShortSkirt*: The attribute *lb-ShortSkirt* was also one of the most challenging for the model to learn. The entire procedure for augmenting this attribute and attempting to improve its results has followed the same general approach as for the final results in *hs-BaldHead*. However, the first difference arises during the image generation process. As shown in Table 37, the number of images composing the augmentation is significantly different. While *hs-BaldHead* had a maximum of 391 images in training (1955 images in total to generate for the maximum augmentation), *lb-ShortSkirt* has more than four times that number. This increases the demand for generated images and highlights a different challenge in learning this attribute, as the base number of training images should be able to give some better base scores.

It is worth noting that another key difference in the generation process lies in the `__styles__` wildcards. Several values had to be modified, as the styles, while suitable in all cases for bald individuals, sometimes referenced garments for the lower



Figure 12: Groundtruth and predicted probabilities for *hs-BaldHead* in RAPzs, highlighted in green or red based on classification.

Table 37: Number of *lb-ShortSkirt* train and test images for RAP datasets.

Dataset	# lb-ShortSkirt Train Images	# lb-ShortSkirt Test Images
RAPv1	912	252
RAPv2	1390	354
RAPzs	643	144

part of the body. Since *lb-ShortSkirt* belongs to the "lower body" category, these styles created conflicts. For instance, when instructing the model to generate pedestrians with short skirts and pants, it produced examples not aligned with expectations.

After adjusting the styles, a complete generation was conducted finishing the prompt with "wearing a short skirt" for the attribute. However, upon manually verifying the presence of the attribute in the images for some of the augmented subsets, it was observed that images generated by the model consistently depicted bare legs, whereas those in the dataset were almost always covered, typically by leggings. Consequently, the prompt was modified to "wearing a short skirt with tights or leggings." This updated prompt not only references the primary attribute but also aligns the generation of the rest of the pedestrian's appearance with the examples in the dataset.

The results obtained from this augmentation for each dataset are available in Tables 38, 39, 40. Table 41 summarizes these results. As can be observed, the results obtained for the attribute itself are worse than those for *hs-BaldHead*. In general, since this attribute starts with higher baseline scores, it is more challenging to improve. However, the scores achieved for the attribute are actually lower than in the base case. This suggests that the generated images fail to capture the patterns that the network needs to learn in order to correctly classify the test images.

Table 38: Performance results for data augmentation of *lb-shortSkirt* in RAPv1

% Augmentation	Noise	Aug. Weight	ShortSkirt					All Attributes				
			ma	Acc	Prec	Rec	F1	ma	Acc	Prec	Rec	F1
50	Medium	0.5	81.09	48.77	68.24	63.10	65.57	80.52	68.71	79.94	81.07	80.50
100	Medium	0.5	81.59	52.10	73.85	63.89	68.51	81.17	68.71	79.60	81.46	80.52
200	Medium	0.5	80.93	49.38	69.91	62.70	66.11	81.04	68.67	79.21	81.84	80.51
300	Medium	0.5	79.41	48.70	72.82	59.52	65.50	80.79	68.14	78.61	81.63	80.09
400	Medium	0.5	80.62	51.15	74.64	61.90	67.68	81.04	68.81	79.00	82.33	80.63
500	Medium	0.5	77.47	46.51	74.07	55.56	63.49	81.01	68.64	78.29	82.90	80.53

Table 39: Performance results for data augmentation of *lb-shortSkirt* in RAPv2

% Augmentation	Noise	Aug. Weight	ShortSkirt					All Attributes				
			ma	Acc	Prec	Rec	F1	ma	Acc	Prec	Rec	F1
50	Medium	0.5	79.17	44.56	64.51	59.04	61.65	79.42	67.17	78.00	80.83	79.39
100	Medium	0.5	77.89	42.19	62.50	56.50	59.35	79.24	67.29	78.29	80.70	79.48
200	Medium	0.5	78.70	42.39	60.95	58.19	59.54	79.19	67.68	78.07	81.63	79.81
300	Medium	0.5	77.23	42.58	65.22	55.08	59.72	79.38	67.39	77.56	81.75	79.60
400	Medium	0.5	78.50	44.64	66.45	57.63	61.72	79.31	67.49	77.36	82.21	79.71
500	Medium	0.5	74.85	39.47	64.73	50.28	56.60	79.30	67.44	77.13	82.47	79.71

Table 40: Performance results for data augmentation of *lb-shortSkirt* in RAPzs

% Augmentation	Noise	Aug. Weight	ShortSkirt					All Attributes				
			ma	Acc	Prec	Rec	F1	ma	Acc	Prec	Rec	F1
50	Medium	0.5	72.01	32.83	54.62	45.14	49.43	73.72	65.80	78.21	78.52	78.37
100	Medium	0.5	70.58	30.35	51.69	42.36	46.56	73.83	65.80	77.99	78.74	78.36
200	Medium	0.5	70.14	33.33	64.13	40.97	50.00	73.77	65.84	77.82	78.95	78.38
300	Medium	0.5	68.96	29.47	54.90	38.89	45.53	73.79	65.60	77.49	79.06	78.27
400	Medium	0.5	69.27	29.38	53.27	39.58	45.42	73.85	65.33	76.72	79.50	78.09
500	Medium	0.5	69.11	31.82	63.64	38.89	48.28	73.81	65.60	76.78	79.83	78.28

Table 41: Comparison of F1 on the attribute and F1 on the Dataset for the *lb-ShortSkirt* attribute across RAPv1, RAPv2, and RAPzs datasets for different data augmentation (DA) percentages.

DA (%)	RAPv1		RAPv2		RAPzs	
	F1 Attribute	F1 Dataset	F1 Attribute	F1 Dataset	F1 Attribute	F1 Dataset
50	65.57	80.50	61.65	79.39	49.43	78.37
100	68.51	80.52	59.35	79.48	46.56	78.36
200	66.11	80.51	59.54	79.81	50.00	78.38
300	65.50	80.09	59.72	79.60	45.53	78.27
400	67.68	80.63	61.72	79.71	45.42	78.09
500	63.49	80.53	56.60	79.71	48.28	78.28
Optimized baseline results	68.62	80.30	62.54	79.38	51.30	78.20

In this case, the problem is unlikely to originate from the testing images per se. Unlike the *hs-BaldHead* scenario in RAPzs, where a limited set of test images exacerbates the impact of noise, the substantially larger test set here contains a smaller percentage of it. While it is present, its influence is discernible yet not critically detrimental. An analysis of the failure cases, as illustrated in Figure 13, corroborates this observation.

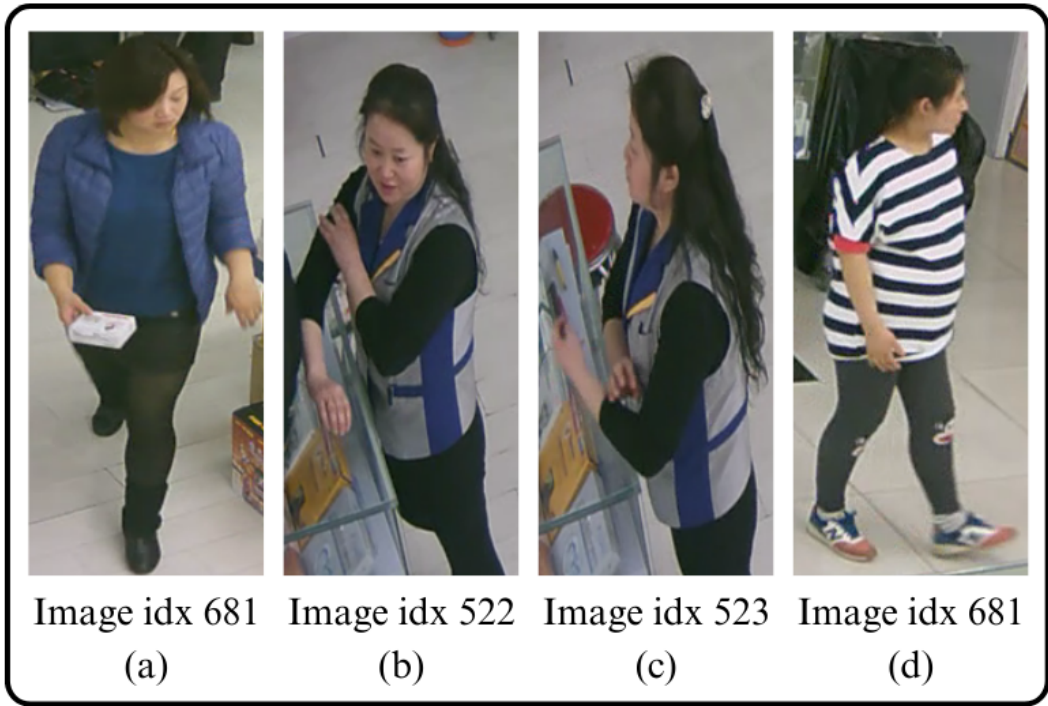


Figure 13: Illustrative examples of challenging cases for the *lb-ShortSkirt* attribute: (a) and (b) present difficulties due to color similarity, (c) requires contextual inference from (b) as it is ambiguous in isolation, and (d) highlights potential labeling inconsistencies.

A significant portion of the test images for this attribute contain short skirts that are challenging to recognize even for human observers. This increases the difficulty of classification, potentially explaining why the baseline model struggles with this attribute, despite having access to a relatively large number of training samples.

This hypothesis is further supported by the learning curves (Figure 14), which show that, across all augmentations, the model continues to improve its performance on the training set, achieving higher accuracy compared to training without augmentation. This suggests that the model is effectively learning from the synthetic images. However, the observed gap between training and test performance indicates overfitting, implying that the learned representations from augmented data do not generalize well to the test set.

However, it is evident that this augmentation fails to resolve the issue associated with the given attribute. Specifically,

Table 42: Number of AgeLess16 train and test images for RAPv1, RAPv2, and RAPzs datasets.

Dataset	# AgeLess16 Train Images	# AgeLess16 Test Images
RAPv1	334	81
RAPv2	603	150
RAPzs	195	68

generations from a general prompt are insufficient in addressing highly specific problems, leading to the inclusion of broader examples that act as distractors within the dataset, ultimately degrading the attribute-specific scores.

Despite the lack of improvement in the targeted attribute, an overall performance gain is observed across the dataset. Given that the baseline for comparison is the previously computed average, one might expect the results to remain unchanged or even deteriorate. However, contrary to this expectation, a positive trend emerges, for instance, RAPv1 exhibits a two-point improvement. This suggests that attributes indirectly influenced by label 3 benefit the model, even though the intended attribute does not generalize well. While the augmentation fails to enhance the specific attribute, it effectively improves the model’s performance on others.

Results on AgeLess16: The third attribute to test is *AgeLess16*, which differs significantly from the previous two as it is the only one that does not refer to something the person is wearing (such as a hairstyle or a piece of clothing), but rather to something the person is. This distinction makes it particularly challenging, as the boundary between *AgeLess16* and the adjacent class, *Age17-30*, is subtle and difficult to define in practice.

To generate samples for this attribute, the objective was to produce pedestrian images without age ambiguity, avoiding cases that could be misclassified as *Age17-30*. Consequently, the chosen prompt emphasized “kid or teenager clearly not older than 15 years old” to ensure the generated individuals were well outside the ambiguous age range.

Following this approach, all required augmentation samples were synthesized, adhering to the values presented in Table 42. In terms of dataset size, this case falls between the previous two: it contains fewer base images than *lb-ShortSkirt*, yet more than *hs-BaldHead*.

After filtering the generated images, a notable observation emerges: despite the prompt containing no explicit reference to pedestrian gender, over 95% of the generated pedestrians were male. This reveals a significant bias in the generative model with the given prompt. To mitigate this issue, an additional generation was conducted by explicitly incorporating the

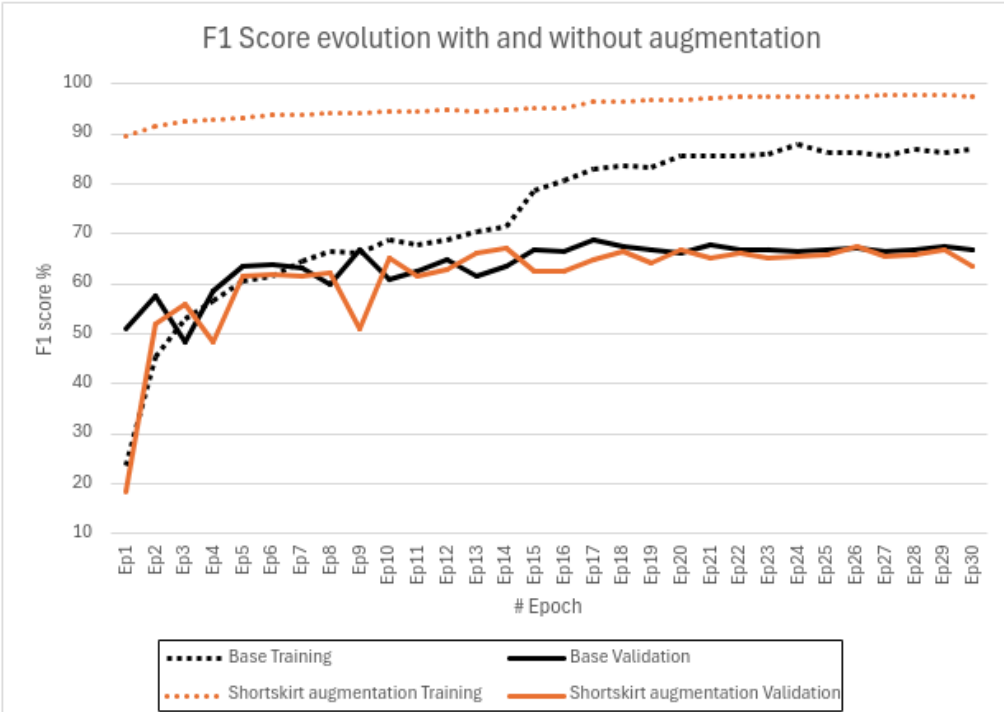


Figure 14: F1 score on *lb-ShortSkirt* during the different epochs of training for the base model and the augmented one.

term female into the prompt. The newly generated images were then alternated with the original set in a one-to-one manner to enhance generalization. Both augmentation sets were subsequently utilized for evaluation, as both had been prepared. Surprisingly, when comparing them, the difference is not significant (an example for RAPv2 can be seen in Figure 15). This may suggest the absence of female children in the evaluation dataset; however, this is not the case. Instead, the model's failure in these instances appears to be influenced by other underlying factors.

All the experiments performed are presented in Tables 43, 44, 45, 46, 47 and 48. A summary is given in Table 49.

Table 43: RAPv1 - AgeLess16 Augmentation Results

% Augmentation	Noise	Aug. Weight	AgeLess16					All Attributes				
			ma	Acc	Prec	Rec	F1	ma	Acc	Prec	Rec	F1
50	Medium	0.5	85.12	61.96	83.82	70.37	76.51	80.36	68.49	79.95	80.75	80.35
100	Medium	0.5	88.83	69.23	86.30	77.78	81.82	80.79	68.25	79.83	80.48	80.15
200	Medium	0.5	85.09	58.76	78.08	70.37	74.03	80.67	68.19	79.20	80.99	80.08
300	Medium	0.5	89.38	62.75	75.29	79.01	77.11	80.80	68.50	79.39	81.27	80.32
400	Medium	0.5	85.15	65.52	90.48	70.37	79.17	80.82	68.63	79.67	81.26	80.46
500	Medium	0.5	85.11	61.29	82.61	70.37	76.00	81.01	68.92	79.57	81.83	80.68

Table 44: RAPv1 - AgeLess16 (with Female) Augmentation Results

% Augmentation	Noise	Aug. Weight	AgeLess16 (with Female)					All Attributes				
			ma	Acc	Prec	Rec	F1	ma	Acc	Prec	Rec	F1
50	Medium	0.5	83.90	61.11	85.94	67.90	75.86	80.49	68.21	79.75	80.45	80.10
100	Medium	0.5	85.73	62.37	82.86	71.60	76.82	80.63	68.34	79.88	80.57	80.22
200	Medium	0.5	86.34	62.77	81.94	72.84	77.12	80.75	68.78	79.51	81.66	80.57
300	Medium	0.5	89.39	64.00	77.11	79.01	78.05	80.82	68.20	79.31	80.99	80.14
400	Medium	0.5	86.36	64.84	85.51	72.84	78.67	80.98	68.70	79.60	81.45	80.51
500	Medium	0.5	84.51	61.54	84.85	69.14	76.19	80.90	68.78	79.54	81.71	80.61

In any case, the general results are presented using the augmentation set that includes *female kids*, as it tends to yield similar results but is considered more general. These results can be found in Table 49. In this case, it is worth highlighting that although the baseline results are relatively high compared to the previous attributes, and thus, one might expect them to remain similar or show only minor improvements, several points of improvement are achieved in the metrics for both RAPv1 and RAPv2. Furthermore, regarding the score for the entire dataset, it is notable that the trend of consistently improving

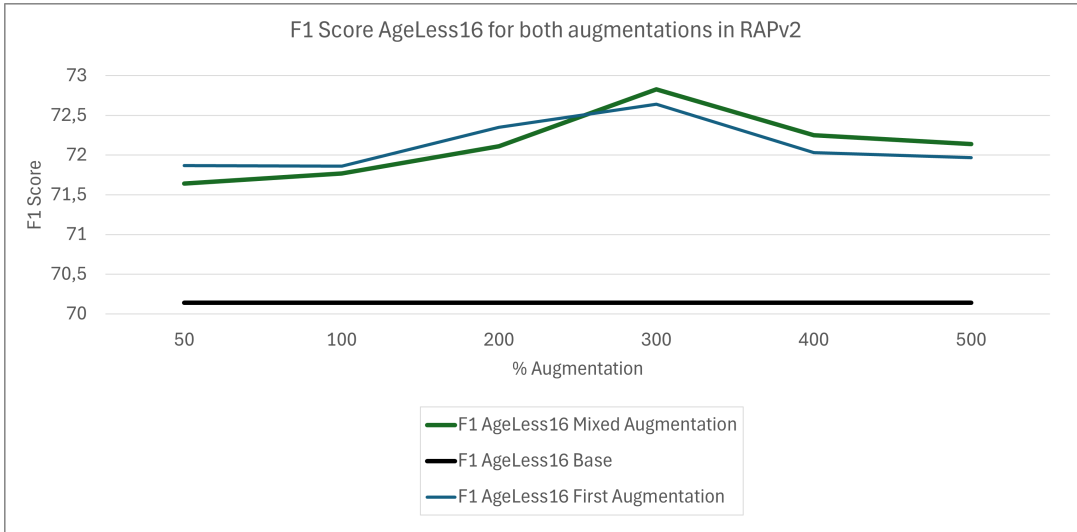


Figure 15: F1 score on RapV2 with the base model, male augmentation (First) and mixed augmentation.

Table 45: RAPv2 - AgeLess16 Augmentation results. Metrics include mean average (ma), accuracy (Acc), precision (Prec), recall (Rec), and F1 score for AgeLess16 and All Attributes under medium noise conditions with varying augmentation percentages.

% Augmentation	Noise	Aug. Weight	AgeLess16					All Attributes				
			ma	Acc	Prec	Rec	F1	ma	Acc	Prec	Rec	F1
50	Medium	0.5	79.77	56.09	74.21	69.68	71.87	78.86	67.39	78.59	80.53	79.54
100	Medium	0.5	80.15	56.08	71.02	72.71	71.86	79.04	67.34	78.16	80.94	79.53
200	Medium	0.5	80.43	56.68	71.97	72.73	72.35	79.17	67.33	78.18	80.92	79.52
300	Medium	0.5	80.91	57.03	70.38	75.04	72.64	79.42	67.48	78.05	81.32	79.65
400	Medium	0.5	80.23	56.28	71.43	72.63	72.03	79.15	67.20	77.73	81.20	79.43
500	Medium	0.5	80.25	56.21	70.94	73.03	71.97	79.25	67.31	77.67	81.48	79.53

Table 46: RAPv2 - AgeLess16 (with Female) Augmentation results

% Augmentation	Noise	Aug. Weight	AgeLess16 (with Female)					All Attributes				
			ma	Acc	Prec	Rec	F1	ma	Acc	Prec	Rec	F1
50	Medium	0.5	79.65	55.81	73.60	69.78	71.64	78.62	67.27	78.53	80.44	79.47
100	Medium	0.5	80.08	55.96	70.92	72.63	71.77	79.20	67.18	77.98	80.87	79.40
200	Medium	0.5	80.21	56.38	72.17	72.05	72.11	79.15	67.35	78.24	80.86	79.53
300	Medium	0.5	81.09	57.27	70.34	75.50	72.83	79.40	67.62	78.16	81.40	79.75
400	Medium	0.5	80.40	56.56	71.64	72.87	72.25	79.12	67.16	77.78	81.14	79.42
500	Medium	0.5	80.31	56.43	71.61	72.69	72.14	79.32	67.51	77.83	81.60	79.67

Table 47: RAPzs - AgeLess16 Augmentation results. Metrics include mean average (ma), accuracy (Acc), precision (Prec), recall (Rec), and F1 score for AgeLess16 and All Attributes under medium noise conditions with varying augmentation percentages.

% Augmentation	Noise	Aug. Weight	AgeLess16					All Attributes				
			ma	Acc	Prec	Rec	F1	ma	Acc	Prec	Rec	F1
50	Medium	0.5	64.62	26.32	71.43	29.41	41.67	72.95	65.34	78.42	77.51	77.96
100	Medium	0.5	70.48	35.44	71.79	41.18	52.34	73.16	65.78	78.56	78.08	78.32
200	Medium	0.5	70.53	37.84	82.35	41.18	54.90	73.50	65.24	77.66	78.17	77.91
300	Medium	0.5	69.76	35.06	75.00	39.71	51.92	73.53	65.19	77.74	78.15	77.94
400	Medium	0.5	70.43	33.73	65.12	41.18	50.45	74.03	65.81	77.85	78.97	78.40
500	Medium	0.5	74.14	41.25	73.33	48.53	58.41	74.19	65.75	77.74	78.95	78.34

it continues. Therefore, overall, the approach also proves to be effective in this case. However, it is important to highlight the situation for the attribute in RAPzs. Unlike the previous two datasets, the attribute itself does not improve, and in some instances, it even worsens considerably. This is notable, particularly given that the same augmentations did yield better results in RAPv1 and RAPv2. This indicates that part of those improved scores are there because the data leakage inherent in the construction of these training and testing sets is behind, as noted by Jia et al. [6]. Additionally, it implies that the augmentation is unable to reproduce the patterns now missing due to the loss of duplicated identities across both subsets, which points to certain characteristics that are difficult to replicate.

By further exploration of the failing cases in the dataset, it is observed that a significant portion of the cases where the classification fails is due to a phenomenon that had not arisen until now. Since children tend to be smaller, the bounding boxes generated around them from the same camera angles are smaller compared to those for adults. Additionally, in many cases, children are not close to the camera, resulting in very small base images that, while interpretable, lose much of the fine-grained details due to image quality, and degrading one of the main features with which we can differentiate the age of a person; the face (Figure 16). As a result, in these cases, the model must rely solely on body shape to determine age, which appears to present some challenges. Furthermore, the model also fails in cases where children are viewed from behind, suggesting a similar issue. This observation makes sense considering the image generation process. In general, generative models often struggle with anatomy and proportions (evident in frequent artifacts like extra or overly long limbs). Although the worst examples of these issues are filtered out during the manual analysis of the generated images, some cases remain

Table 48: RAPzs - AgeLess16 (with Female) Augmentation Results

% Augmentation	Noise	Aug. Weight	AgeLess16 (with Female)					All Attributes				
			ma	Acc	Prec	Rec	F1	ma	Acc	Prec	Rec	F1
50	Medium	0.5	65.39	28.77	80.77	30.88	44.68	73.06	65.37	78.50	77.51	78.00
100	Medium	0.5	67.56	31.58	75.00	35.29	48.00	72.95	65.60	78.36	77.96	78.16
200	Medium	0.5	71.97	38.96	76.92	44.12	56.07	73.67	65.09	77.48	78.13	77.80
300	Medium	0.5	73.44	41.56	78.05	47.06	58.72	74.12	65.64	77.73	78.85	78.29
400	Medium	0.5	69.78	36.00	79.41	39.71	52.94	73.98	65.95	77.94	79.08	78.51
500	Medium	0.5	74.10	39.29	67.35	48.53	56.41	74.14	65.74	77.69	78.99	78.33

Table 49: Comparison of F1 on the Attribute and F1 on the Dataset for the *AgeLess16* attribute across RAPv1, RAPv2, and RAPzs datasets for different data augmentation (DA) percentages.

DA (%)	RAPv1		RAPv2		RAPzs	
	F1 Attribute	F1 Dataset	F1 Attribute	F1 Dataset	F1 Attribute	F1 Dataset
50	75.86	80.10	71.64	79.47	44.68	78.00
100	76.82	80.22	71.77	79.40	48.00	78.16
200	77.12	80.57	72.11	79.53	56.07	77.80
300	78.05	80.14	72.83	79.75	58.72	78.29
400	78.67	80.51	72.25	79.42	52.94	78.51
500	76.19	80.61	72.14	79.67	56.41	78.33
Optimized baseline results	75.82	80.30	70.14	79.38	59.02	78.20

where the images, while clearly depicting children based on facial features, have body shapes that might resemble those of adults or fall somewhere in between.

This finding makes classification based on body shape a challenge, especially given the wide range of body types within the age category, encompassing infants, young children, preteens, and teenagers. Regulating this issue with text-to-image generation is challenging, so further improvements for this attribute using this approach depend heavily on the generative precision of the model. Nonetheless, given that results are improved in the first two datasets, it can be concluded that no noise is being introduced into the dataset in any case.



Figure 16: Examples of challenging cases for the *AgeLess16* attribute: (a), (b), and (c) depict individuals with poor image quality due to resizing, showing back, side, and front views respectively, where (b) and (c) lose facial details. (d) shows a pedestrian with ambiguous age characteristics.

Table 50: Number of ub-SuitUp train and test images for RAP datasets.

Dataset	# hs-SuitUp Train Images	# hs-SuitUp Test Images
RAPv1	716	205
RAPv2	2067	525
RAPzs	461	112

Table 51: Comparison of F1 on the Attribute and F1 on the Dataset for the *ub-SuitUp* attribute across RAPv1, RAPv2, and RAPzs datasets for different data augmentation (DA) percentages.

DA (%)	RAPv1		RAPv2		RAPzs	
	F1 Attribute	F1 Dataset	F1 Attribute	F1 Dataset	F1 Attribute	F1 Dataset
50	67.70	80.14	65.50	79.72	64.25	78.46
100	68.42	80.41	66.87	79.55	67.94	78.19
200	67.02	80.42	64.55	79.64	63.68	78.09
300	66.99	80.29	65.07	79.63	66.02	78.31
400	68.25	80.66	66.00	79.62	65.37	78.19
500	66.30	80.45	63.19	79.79	68.32	78.32
Optimized baseline results	69.29	80.30	65.83	79.38	66.67	78.20

Table 52: Number of attach-PaperBag train and test images for RAP datasets.

Dataset	# attach-PaperBag Train Images	# attach-PaperBag Test Images
RAPv1	397	129
RAPv2	704	181
RAPzs	197	54

Results on ub-SuitUp: Following the unsuccessful outcomes with lb-ShortSkirt, ub-SuitUp becomes an attribute of particular interest, as it features an even higher number of training images, as can be seen in Table 50.

Following the experiments, our findings reveal that the specific attribute in question has indeed been enhanced (Table 51). This outcome contrasts with the behavior observed in the lb-ShortSkirt case, where such improvement was absent, thereby eliminating the possibility that the number of images directly influenced the obtained results. However, in the case of ub-SuitUp, a novel behavior emerges: while both RAPv2 and RAPzs improve, RAPv1 experiences a decline. Given that RAPv2 encompasses RAPv1, the decrease in RAPv1 is of lesser concern. Although pinpointing why improvements are isolated to RAPv2 and RAPzs remains challenging, even if it proves that the proposed approach does not introduce noise. Moreover, the enhancement observed in the zero-shot variant of the datasets is particularly significant; it deviates from the patterns seen with previous attributes and indicates that incorporating synthetic data enhances generalization under these conditions. When evaluating the metrics on the complete dataset, we can observe again consistent improvements. These gains are more pronounced at higher augmentation percentages, although peaks in performance may occur at specific augmentation levels.

Results on attach-PaperBag: The attribute attach-PaperBag exhibits a number of images comparable to most attributes in the dataset (see Table 52); however, its baseline performance remains considerably low. This behavior may be attributed to its similarity to other attributes in the same category, particularly attach-PlasticBag.

As can be seen, our experiments on the attribute (Table 53) demonstrates a compelling use-case of the proposed approach. By integrating data augmentation within the attribute module, we observe notable performance gains on both the official datasets and their zero-shot variants. These improvements are evident at both the attribute and dataset levels, underscoring the efficacy of the method.

Moreover, the attribute recognition results on RAPzs capture one of the primary goals of our work: enhancing the detection of underrepresented attributes in zero-shot scenarios.

Overall Performance: After optimizing augmentation per attribute, we tested simultaneous augmentation across datasets. We evaluated two models: one using 500% augmentation for all attributes and another applying each attribute’s optimal augmentation level. Since *lb-ShortSkirt* showed no improvement, we also tested augmentation with only *hs-BaldHead* and *AgeLess16*. Table 54 presents the average results over 10 runs.

As observed, even when directly augmenting only 2 or 3 attributes out of 52, and indirectly enhancing a small additional

Table 53: Comparison of F1 on the Attribute and F1 on the Dataset for the *attach-PaperBag* attribute across RAPv1, RAPv2, and RAPzs datasets for different data augmentation (DA) percentages.

DA (%)	RAPv1		RAPv2		RAPzs	
	F1 Attribute	F1 Dataset	F1 Attribute	F1 Dataset	F1 Attribute	F1 Dataset
50	51.35	80.17	41.48	79.52	17.72	78.21
100	51.10	80.45	41.09	79.62	20.93	78.27
200	49.54	80.33	40.00	79.79	25.88	78.10
300	54.17	80.27	41.64	79.75	33.33	78.04
400	45.37	80.52	44.14	79.80	30.93	78.35
500	49.28	80.43	45.14	79.63	23.38	78.19
Optimized baseline results	45.79	80.30	42.90	79.38	9.30	78.20

Table 54: Performance comparison with updated results over RAPv1, RAPv2, and RAPzs.

Condition	% Aug.	RAPv1					RAPv2					RAPzs				
		mA	Acc	Prec	Rec	F1	mA	Acc	Prec	Rec	F1	mA	Acc	Prec	Rec	F1
Augmenting hs-BaldHead & AgeLess16	500% Augmentation	80.94 ±0.18	68.66 ±0.14	79.14 ±0.06	81.93 ±0.23	80.51 ±0.11	79.45 ±0.07	67.33 ±0.10	77.31 ±0.13	82.01 ±0.11	79.59 ±0.07	73.65 ±0.18	65.50 ±0.13	77.38 ±0.14	78.95 ±0.13	78.16 ±0.11
	Best F1 Augmentation	80.79 ±0.18	68.52 ±0.12	79.15 ±0.12	81.64 ±0.11	80.38 ±0.08	79.13 ±0.07	67.63 ±0.09	77.86 ±0.13	81.78 ±0.12	79.77 ±0.07	73.65 ±0.18	65.50 ±0.13	77.38 ±0.14	78.95 ±0.13	78.16 ±0.11
Augmenting all	500% Augmentation	81.14 ±0.12	68.64 ±0.11	77.90 ±0.09	83.51 ±0.21	80.60 ±0.09	79.75 ±0.12	67.27 ±0.11	75.87 ±0.12	83.87 ±0.08	79.67 ±0.08	74.57 ±0.16	65.93 ±0.14	75.89 ±0.14	81.56 ±0.30	78.62 ±0.11
	Best F1 Augmentation	81.01 ±0.18	68.63 ±0.16	78.80 ±0.11	82.29 ±0.14	80.50 ±0.11	79.67 ±0.12	67.47 ±0.10	76.51 ±0.07	83.30 ±0.15	79.76 ±0.08	73.89 ±0.13	65.93 ±0.12	76.95 ±0.09	80.16 ±0.21	78.52 ±0.10
Optimized baseline results	-	80.54 ±0.17	68.49 ±0.10	79.89 ±0.08	80.72 ±0.13	80.30 ±0.08	79.12 ±0.10	67.17 ±0.10	78.35 ±0.09	80.43 ±0.12	79.38 ±0.09	74.39 ±0.22	65.59 ±0.23	78.19 ±0.15	78.20 ±0.27	78.20 ±0.19

subset through the proposed augmented loss, results improved across all datasets.

It is noteworthy that including lb-ShortSkirt in the augmentations tends to be beneficial, as this variation either achieves the best results or very competitive ones. Conversely, omitting it occasionally seems to result in losing the extra boost provided by the indirectly augmented attributes from those images.

Additionally, precision is the only metric that does not show improvement, suggesting that the model exhibits a tendency to classify the augmented classes as positive more frequently, even in cases of incorrect predictions. This aligns with the challenges observed in fully resembling the dataset. Nevertheless, the overall improvement is indisputable, indicating that a generation approach tailored to address specific challenges within the dataset, and/or the augmentation of most or all attributes rather than a limited subset, can lead to significant improvements.

E. ComfyUI configuration

E.1. ComfyUI - Generation Process Description

For the generation process, once the flow was constructed, the decision was made to ensure that all generations were replicable. This involved using the same seed, "123456789," across the *KSampler*, *NoiseGenerator*, and *PromptSampler*, incrementing it for each subsequent generation. However, it appears that the *PromptSampler*, being a custom node, does not handle this functionality correctly, and the seed remains static unless set to random mode.

For this reason, the procedure has been maintained for the *KSampler* and *NoiseGenerator*, while the *PromptSampler* has been left in random mode. Nonetheless, all the generated prompts have been recorded, ensuring that, with these prompts and the corresponding seeds, the images can be reproduced. With this setup, the generations were carried out. For each attribute, more images than necessary were always generated, as those that either did not contain the attribute or exhibited significant generation errors were manually discarded. For reproducibility, the index of all discarded images have also been saved, which represent a greater or lesser percentage depending on the attribute.

Finally, it is important to note that the decision was made to perform the generation process in a distributed manner. Throughout this project, more than double the number of images specified in this report had to be generated.

To maintain the reproducibility specified earlier, the seeds were recalculated for each batch. The first image of the first batch always started with the seed 123456789, and the seed for the first image of each subsequent batch was calculated by adding the batch size to the batch number, according to Equation 3.

$$\text{Seed}_{\text{batch},1} = \text{Seed}_{\text{initial}} + (\text{Batch Size} \times (\text{Batch Number} - 1)) \quad (3)$$

E.2. ComfyUI Workflow Details

The following describes the *ComfyUI* flow used for image generation. The various nodes are grouped into modules, with their inputs (if applicable) and parameters specified.

LOAD MODELS

– Load Checkpoint

```
parameters:  
    ckpt_name = sd3_medium_incl_clips_t5xxlfp8.safetensors
```

– TripleCLIPLoader

```
parameters:  
    clip_name1 = clip_g.safetensors  
    clip_name2 = clip_l.safetensors  
    clip_name3 = t5xxl_lp16.safetensors
```

INPUT

– EmptySD3LatentImage

```
parameters:  
    width = 2784  
    height = 1024  
    batch_size = 1
```

– Random Prompts [31]

```
parameters:
```

```
text = <prompt>
seed = 123456789
control_after_generate = randomize
autorefresh = No
```

- CLIP Text Encode (Prompt)

```
inputs:
  clip = TripleCLIPLoader
  text = Random Prompts
```

- CLIP Text Encode (Negative Prompt)

```
inputs:
  clip = TripleCLIPLoader
parameters:
  text = <negative prompt>
```

- Show Text Value

```
inputs:
  text = Random Prompts
parameters:
  split_lines = false
```

- Save Text

```
inputs:
  text = Show Text Value
parameters:
  filename_prefix = 1_ComfyUI
  images_paths = None
```

GENERATION STEPS

- ModelSamplingSD3

```
inputs:
  model = Load Checkpoints
parameters:
  shift = 3.00
```

- ConditioningZeroOut

```
inputs:
  conditioning = CLIP Text Encode (Negative Prompt)
```

- ConditioningSetTimestepRange

```
inputs:
  conditioning = CLIP Text Encode (Negative Prompt)
parameters:
```

```
    start = 0.000
    end = 0.100
```

– **ConditioningSetTimestepRange**

```
inputs:
    conditioning = ConditioningZeroOut
parameters:
    start = 0.100
    end = 1.000
```

– **Conditioning (Combine)**

```
inputs:
    conditioning_1 = ConditioningSetTimestepRange
    conditioning_2 = ConditioningSetTimestepRange
```

– **KSampler**

```
inputs:
    model = ModelSamplingSD3
    positive = CLIP Text Encode (Prompt)
    negative = Conditioning (Combine)
    latent_image = EmptySD3LatentImage
parameters:
    seed = 123456789
    control_after_generate = increment
    steps = 28
    cfg = 4.5
    sampler_name = dpmpp_2m
    scheduler = sgm_uniform
    denoise = 1.00
```

– **VAE Decode**

```
inputs:
    samples = KSampler
    vae = Load Checkpoint
```

POSTPROCESSING

– **ToolYoloCropper** [32], [33]

```
inputs:
    image = VAE Decode
parameters:
    object = person
    padding = 0
```

– **Greyscale Noise** [34]

```
parameters:
```

```
width = 1024
height = 1024
value_min = -1
value_max = -1
red_min = -1
red_max = -1
green_min = -1
green_max = -1
blue_min = -1
blue_max = -1
seed = 123456789
control_after_generate = increment
```

- **ImageBlend**

```
inputs:
  image1 = ToolYoloCropper
  image2 = Greyscale Noise
parameters:
  blend_factor = 0.25
  blend_mode = soft_light
```

- **Upscale Image By [35]**

```
inputs:
  image = ImageBlend
parameters:
  upscale_method = nearest-exact
  scale_by = 0.33
```

- **Upscale Image By**

```
inputs:
  image = Upscale Image By
parameters:
  upscale_method = bilinear
  scale_by = 3.00
```

- **ImageBlur**

```
inputs:
  image = Upscale Image By
parameters:
  blur_radius = 5
  sigma = 0.4
```

- **Brightness & Contrast**

```
inputs:
  image = ImageBlur
```

```
parameters:  
    contrast = 0.80  
    brightness = 0.90
```

OUTPUT

– Save Image

```
inputs:  
    images = Brightness & Contrast  
parameters:  
    filename_prefix = ComfyUI
```

Supplementary References

- [30] J. Jia *et al.*, “Rethinking of pedestrian attribute recognition: A reliable evaluation under zero-shot pedestrian identity setting,” *arXiv:2107.03576*, 2021.
- [31] Adieyal, “Comfyui dynamicprompts: Comfyui custom nodes for dynamic prompts,” 2024, accessed: 2024-12-18. [Online]. Available: <https://github.com/adieyal/comfyui-dynamicprompts>
- [32] tooldigital, “Comfyui-yolo-cropper: A simple comfyui node for image cropping and masking using yolov8,” 2024, accessed: 2024-12-21. [Online]. Available: <https://github.com/tooldigital/ComfyUI-Yolo-Cropper>
- [33] R. Varghese and S. M., “Yolov8: A novel object detection algorithm with enhanced performance and robustness,” in *2024 International Conference on Advances in Data Engineering and Intelligent Computing Systems (ADICS)*, 2024, pp. 1–6.
- [34] Jordach, “Comfy-plasma: A simple plasma noise generator for comfyui,” 2024, accessed: 2024-12-21. [Online]. Available: <https://github.com/Jordach/comfy-plasma>
- [35] W. Palant, “Image resize for comfyui: A custom node providing various tools for resizing images without distorting proportions,” 2024, accessed: 2024-12-21. [Online]. Available: <https://github.com/palant/image-resize-comfyui>